Dyslipidemia, metabolism and autophagy : antigen-independent modulation of T cells in atherosclerosis

Amersfoort, J.

CHAPTER 3

Diet-induced dyslipidemia induces metabolic and migratory adaptations in regulatory T cells

Manuscript submitted for publication

J. Amersfoort[1]
H. Douna[1]
F.H. Schaftenaar[1]
P.J. van Santbrink[1]
G.H.M. van Puijvelde[1]
B. Slütter[1]
A.C. Foks[1]
A. Harms[2]
E. Moreno-Gordaliza[2]
Y. Wang[3]
T. Hankemeier[2]
I. Bot[1]
H. Chi[3]
J. Kuiper[1]

[1]Division of BioTherapeutics, LACDR, Leiden University, Leiden, The Netherlands
[2]Division of Biomedicine and Systems Pharmacology, LACDR, Leiden University, Leiden, The Netherlands
[3]Department of Immunology, St. Jude Children's Research Hospital, Memphis TN, USA

ABSTRACT

A hallmark of advanced atherosclerosis is inadequate immunosuppression by regulatory T (Treg) cells inside the atherosclerotic lesion. Here we show that this impairment is not due to a reduction in migratory capacity of Treg cells as diet-induced dyslipidemia, one of the major risk factors for atherosclerosis, actually skewed their migration towards sites of inflammation instead of lymph nodes. Mechanistically, we discovered that diet-induced dyslipidemia altered mTOR signaling and induced PPARδ activation, thereby increasing fatty acid (FA) oxidation in Treg cells. Treatment with a synthetic PPARδ agonist increased the migratory capacity of Treg cells in an FA oxidation dependent manner. Furthermore, diet-induced dyslipidemia enhanced Treg cell influx into atherosclerotic lesions indicating that enhanced FA oxidation drives Treg cell migratory function during atherosclerosis. Altogether, our findings implicate that a decrease in Treg cell immunosuppression is not due to impairment in their migratory capacity but due to an unfavorable microenvironment inside atherosclerotic lesions.

KEYWORDS

Dyslipidemia, atherosclerosis, Treg cell, mTOR, PPARδ, migration

INTRODUCTION

Dyslipidemia as exemplified by hypercholesterolemia and/or hypertriglyceridemia is a driving force for the development of atherosclerosis. Atherosclerosis is an autoimmune-like disease affecting the arterial wall in which (modified) lipoproteins such as low-density lipoprotein (LDL) accumulate in the subendothelial space and elicit an adaptive immune response involving $CD4^+$ T cells [1]. Regulatory T (Treg) cells represent a subset of $CD4^+$ T cells which maintains tolerance to self-antigens and regulates inflammation to dampen tissue damage [2]. Treg cells are thus considered a promising therapeutic target to treat autoimmune-like disorders, including atherosclerosis [3]. Accordingly, as Treg cell abundancy is low in advanced atherosclerotic lesions in mice [4] and humans [5–7], a local loss of tolerance to lipoproteins is speculated to be causal in atherosclerosis progression. Previously, it has been shown that the capacity of splenic Treg cells to bind to activated endothelium is inversely related to the degree of diet-induced dyslipidemia and this may be due to a decreased expression of ligands for P- and E-selectin on Treg cells [4]. Thereby, fewer Treg cells which egress from secondary lymphoid organs (SLOs) and enter the circulation would subsequently migrate towards atherosclerotic lesions, thereby contributing to a local loss of tolerance.

In the last decade, intricate adaptations in the metabolism of glucose and lipids have been shown to be crucial for Treg cells to properly exert their function during inflammation [8–11]. Recently, it was discovered that Treg cells require glycolysis to generate sufficient ATP for their migration [12]. Interestingly, inhibition of the glycolytic enzyme PFKFB3 in $CD4^+$ T cells has been shown to induce ATP-depletion, which causes lipid droplet formation and activates the transcriptional program for migratory machinery, thereby generating pro-inflammatory, tissue invasive T cells [13]. Thus, cellular metabolism affects T cell migration in different manners. Whether dyslipidemia causes adaptations in cellular metabolism in Treg cells inside SLOs and whether this affects their migration in the context of atherosclerosis has not yet been investigated.

It seems feasible that dyslipidemia affects cellular metabolism in Treg cells as cholesterol accumulation in ATP-binding cassette G1 (ABCG1)-deficient Treg cells inhibits mammalian target of rapamycin complex 1 (mTORC1) [14]. mTORC1 is a protein complex in which the kinase mTOR can regulate cellular metabolism by promoting glycolysis in activated T cells through its downstream targets hypoxia inducible factor-1α (HIF1α) and Myc [15,16]. Moreover, mTORC1 inhibits fatty acid (FA) oxidation, possibly by inhibiting the rate-limiting enzyme carnitine-palmitoyl transferase 1A (Cpt1a) [17,18].

Furthermore, diet-induced dyslipidemia likely also affects Treg cell migration through a distinct mechanism. Specifically, obesity-induced metabolic stress primes $CD4^+$ T cells to acquire an effector phenotype by altering the activity of the PI3K-p110δ-Akt kinase signaling pathway upon activation. This alteration lowers the expression of CD62L and

C-C chemokine receptor type 7 (CCR7) [19] which are membrane-associated proteins involved in the homing of T cells to lymph nodes (LN) through high endothelial venules. Hence, these reports indicate that key regulators of cellular metabolism and migration in T(reg) cells can be affected by perturbations in the levels of extra- and intracellular lipids.

In this paper we investigated the dyslipidemia-induced effects on migration and cellular metabolism in Treg cells. Mechanistically, we discovered that dyslipidemia induced intrinsic changes in mTORC2 signaling, inhibited mTORC1 and glycolysis but increased FA oxidation in Treg cells. We furthermore showed that the latter was not entirely mTORC1 mediated. Mass spectrometry analysis of dyslipidemic serum uncovered increases in peroxisome proliferator activated receptor delta (PPARδ) ligands, which contributed to increased FA oxidation in Treg cells. Dyslipidemia also increased the capacity of Treg cells to migrate towards sites of inflammation and the PPARδ agonist GW501516 increased their migration in an FA oxidation-dependent manner indicating that diet-induced dyslipidemia can affect Treg cell migration partly by skewing their metabolism.

MATERIALS & METHODS

Mice

Wildtype C57BL/6J mice and LDL-receptor deficient B6.129S7-Ldlrtm1Her/J (*Ldlr*$^{-/-}$) mice were purchased from the Jackson Laboratory and further bred in the Gorlaeus Laboratory in Leiden, The Netherlands. Diet-induced dyslipidemia and atherosclerosis were established by feeding *Ldlr*$^{-/-}$ mice from 9-12 weeks of age a Western-type diet (WTD) containing 0.25% cholesterol and 15% cocoa butter (Special Diet Services) for 16-20 weeks. At sacrifice, the mice were sedated and their blood was collected via orbital blood collection. Subsequently, their vascular system was perfused with PBS at a continuous low flow via heart puncture in the left ventricle after which the spleens and lymph nodes were collected for further processing. Apolipoprotein E deficient B6.129P2-Apoetm1Unc/J (*Apoe*$^{-/-}$) mice were purchased from the Jackson Laboratory and at 20 weeks of age were fed a WTD for 8 weeks to promote atherosclerosis formation. *Apoe*$^{-/-}$ mice were sacrificed similar to LDLr$^{-/-}$ mice and the aortic arch and thoracic aortas were harvested additionally. B6.SJL-PtprcaPepcb/BoyCrl (CD45.1) mice were purchased from Charles River. The animals were kept under standard laboratory conditions and were fed a normal chow diet (NCD) and water *ad libitum*. All animal work was performed according to the guidelines of the European Parliament Directive 2010/63EU and the experimental work was approved by the Animal Ethics committee of Leiden University.

Flow cytometry

Spleens and lymph nodes were mashed through a 70 µm cell strainer after isolation. Erythrocytes were subsequently eliminated from the splenocyte suspension by incubating the cells with ACK erythrocyte lysis buffer to generate a single-cell suspension prior to staining of surface markers. Blood samples were also lysed with ACK erythrocyte lysis buffer to prepare them for staining. For the staining of surface markers, cells were stained at 4°C for 30 minutes in staining buffer (PBS with 2% (vol/vol) fetal bovine serum (FBS)) in which we diluted the antibodies. Intracellular transcription factors were stained for by following the FoxP3 staining protocol (eBioscience). All antibodies used for staining of surface markers or transcription factors were from eBioscience, BD Biosciences or BioLegend (table 1). For staining of unesterified cholesterol, lymphocytes were stained after surface staining with 50µg/mL filipin III (Cayman) at room temperature for 45 minutes and subsequently washed with PBS twice before sample analysis. For staining of lipid droplets using BODIPY^{TM} 493/503 (Invitrogen), cells were stained with 1,3µg/mL BODIPY in pre-warmed PBS at room temperature for 10 minutes. For staining of mitochondria, lymphocytes were incubated with 10 nM MitoTracker Deep Red (Life Technologies) for 30 minutes at 37°C. To stain for Glut1, cells were fixed in 1% formaldehyde and incubated overnight in 100% methanol at -80°C. Subsequently, the cells were washed with PBS with 2% FCS, incubated with blocking solution and subsequently incubated with anti-Glut1 antibody (Abcam) at room temperature for 1h. After extensive washing, the cells were stained for 30 min. at room temperature with antibodies for surface markers and a goat-anti-rabbit antibody conjugated to allophycocyanin (Abcam). All samples were washed with staining buffer and resuspended in staining buffer prior to flow cytometric analysis.

Flow cytometric analysis was performed on a FACSCantoII (BD Biosciences) or a Cytoflex S (Beckman Coulter) and data was analyzed using Flowjo software (TreeStar).

Phosflow analysis

For detection of phosphorylated signaling proteins using flow cytometry, splenocytes from NCD or WTD fed mice or diet-switch mice were rested in complete RPMI-1640 for 2h. After this, splenocytes were stimulated with 100U/mL of recombinant IL-2 (Peprotech) prior to staining for surface markers on ice in the dark for 30 minutes. A control without IL-2 induced stimulation of the mTORC1 and mTORC2 pathways was used. Stimulation was followed by fixation with BD Phosflow™ Lyse/Fix Buffer (BD Biosciences), subsequent permeabilization with Phosflow Perm buffer III (BD Biosciences) and staining with Alexa Fluor® 488-conjugated phospho-S6 (Ser235/236), Alexa Fluor® 647-conjugated phospho-4E-BP1 (Thr37/46) (Cell Signaling Technologies) or V450 conjugated phospho-Akt (Ser473) antibodies (BD Biosciences) at room temperature for 1h. The cells were then washed and prepared for flow cytometric analysis.

Cell culture

$CD4^+$ T cells or $CD4^+CD25^+$ Treg cells were isolated from spleens from $LDLr^{-/-}$ mice using MACS microbeads (Miltenyi Biotec). Samples were excluded when the purity was below 93% as assessed by flow cytometry. Alternatively, Treg cells were flow sorted on a FACS Aria III by gating on viable $CD3^+CD4^+CD25^{hi}$ cells. Treg cells were stimulated using plate-coated anti-CD3e (5µg/mL; Ebioscience), anti-CD28 (0,5µg/mL; Ebioscience) and 200U/mL recombinant mIL-2 (Peprotech) and cultured in RPMI-1640 supplemented with 2 mM L-glutamine, 100U/mL pen/strep and 10% FBS (all from Lonza). For *in vitro* experiments, Treg cells were isolated from the spleen, mediastinal, mesenteric and inguinal lymph nodes using MACS microbeads or flow sort. *In vitro* lipid loading experiments were performed by supplementing culture medium with 10% mouse serum from $LDLr^{-/-}$ mice with normolipidemia or dyslipidemia. Alternatively, lipid loading was achieved by culturing Treg cells with β-very low density lipoprotein particles which were isolated from rat serum through KBr density gradient ultracentrifugation. GW501516 (Enzo Life Sciences) was used at 0.1µM in complete RPMI-1640 with 10 mM D-glucose. Dimethyl sulfoxide (DMSO) was used as a vehicle control in the GW501516 compound experiments. For the GSK compound study, GSK0660 (Sigma) was used *in vitro* on isolated NCD- and WTD-Treg cells under plate-coated anti-CD3e, anti-CD28 and 200U/mL recombinant mIL-2 stimulation for 4 hours at a concentration of 1µM. DMSO was used as a vehicle control. Rapamycin (LC Laboratories) was used at a concentration of 100 nM and DMSO was used as a vehicle control.

RNA and immunoblot analysis

mRNA was extracted from freshly isolated or cultured Treg cells using the guanidium isothiocyanate (GTC) method after which cDNA was generated using RevertAid M-MuLV reverse transcriptase per manufacturer's instructions (Thermo Scientific). Quantitative gene expression analysis was performed using Power SYBR Green Master Mix on a 7500 Fast Real-Time PCR system (Applied Biosystems). Gene expression was normalized to 2-3 housekeeping genes (table 1). Immunoblots were performed and quantified as described previously[8], using the following antibodies: p-S6, p-Foxo1 (all from Cell Signaling Technology), HIF1α (Cayman Chemical) and β-actin (Sigma). Immunoblot results were quantified using Fiji biological-image analysis software.

FA oxidation assay

Freshly isolated or cultured Treg cells were resuspended in minimal DMEM supplemented with 10 mM D-glucose (Sigma), 2mM L-glutamine (Lonza), 10% FBS, HEPES, sodium bicarbonate and 5µCi [9,10-^{3}H]-palmitic acid (PA) (Perkin Elmer). Cells were incubated for 2h (unless otherwise stated) at 37°C after which the supernatant was transferred to 1.5 mL microcentrifuge tubes. After centrifugation, the supernatant was transferred to

20ml scintillation vials which were sealed with a rubber stopper containing Whatmann filtration paper pre-equilibrated in milliQ. After 48 hours of incubation at 37°C, the Whatmann filtration paper containing the metabolized ^3H_2O was harvested. Per assay, three cell-free samples containing only 5µCi [9,10-^{3}H]-PA were used as a background control. Mitochondrial FA oxidation (simply referred to as FA oxidation) was determined by the difference between the oxidation rate in the absence or presence of 100µM etomoxir (Sigma).

Metabolic flux assay

Oxygen consumption rate (OCR) and extracellular acidification rate (ECAR) were measured using an XF96e Extracellular Flux Analyzer (Seahorse Bioscience). Freshly isolated Treg cells were stimulated with plate-bound anti-CD3e, soluble anti-CD28 and IL-2 for 4h. After this, Treg cells were replated in XF medium (nonbuffered DMEM supplemented with 10 mM glucose, 2mM L-glutamine and 1 mM sodium pyruvate). An XF96e Extracellular Flux Analyzer was used to measure OCR and ECAR in response to 1µM oligomycin, 1µM FCCP, 1.25 µM rotenone, 2.5 µM antimycin A and 100 mM 2-deoxyglucose (all from Sigma).

Treg cell peritoneum migration

Treg cell peritoneal homing experiments were based on Fu et al [50]. Briefly, CD45.1 mice were injected i.p. with 600U interferon gamma (Ebioscience) 72h prior to an i.v. adoptive transfer of $15x10^6$ CD45.2 $CD4^+$ T cells or $1.5x10^6$ $CD45.2^+CD4^+CD25^+$ Treg cells. After 16-18 hours, the mice were sacrificed and peritoneal cells were collected by performing a peritoneal lavage and the spleen and mesenteric lymph nodes were excised. Peritoneal cells, splenocytes and lymphocytes were subsequently used for flow cytometry detection of $CD45.2^+$ Treg cells.

Aorta influx

In vitro Treg cell homing was assessed by adapting a protocol from Li et al. [43]. The aortic arch and thoracic aorta were surgically removed from WTD-fed *Apoe*$^{-/-}$ mice with atherosclerosis and dissected transversally into six pieces. Freshly isolated Treg cells from the spleens of mice which were fed an NCD or WTD were pooled in an NCD and a WTD fraction and subsequently labeled with 5 µM CellTrace™ Violet (Invitrogen) as per manufacturer's instructions. After this, the NCD- and WTD-Treg cell fractions were split in two and were treated with 100µM etomoxir or maintained in medium for 1h. After incubation, the cells were washed and counted using a hemocytometer before adding 200,000 Treg cells per aorta. The Treg cells were left to migrate overnight in complete RPMI-1640 with 10 mM D-glucose. Subsequently, the aortic fragments were washed extensively in ice-cold PBS containing 2% FCS and 2 mM EDTA. After this, the aortic fragments were

cut up into small pieces and digested by incubating them with a digestion mix containing 450 U/mL collagenase I, 250 U/mL collagenase XI, 120 U/mL DNAse and 120 U/mL hyaluronidase (all from Sigma) for 30 minutes at 37˚C under agitation. Subsequently, the digested aortas were strained over a 70-µm strainer to prepare them for antibody staining for flow cytometry to detect migrated Treg cells.

Transmigration assay

Treg cells were treated with 0.1µM GW501516 or vehicle for 16-18h in complete RPMI supplemented with 10 mM glucose. Subsequently, Treg cells were treated with 100 µM etomoxir for 1 hour and then seeded into transwell tissue culture well inserts (5µm pore-size) and left to migrate towards 250 ng/mL CCL21 (Peprotech) for 6-8 hours. The number of migrated cells was determined manually using a hemocytometer. The results are depicted as a percentage of migrated cells.

Serum analysis

Concentrations of total cholesterol and triglycerides in the serum were determined by an enzymatic colorimetric assay (Roche Dagnostics). Precipath (standardized serum, Roche Diagnostics) was used as an internal standard. Concentrations of free fatty acids in the serum were quantified using the Free Fatty Acid Quantification Kit (Sigma) as per manufacturer's instructions. For measurement of blood glucose levels, mice were fasted for 4 hours prior to blood collection. Blood samples were taken from the tail vein and directly applied to an Accu-Check glucometer (Roche Diagnostics).

Serum lipidomics

Ldlr$^{-/-}$ mice were fed a WTD or maintained on an NCD for 8 weeks and upon sacrifice, serum samples were collected and frozen at -80˚C until use. The operating procedures of the targeted lipidomics platform are optimized from the previously published method [51]. Polar lipids are extracted using methanol to precipitate proteins from serum samples and this method covers low abundance lipid species, including free fatty acids and lysophospholipids—lysophosphatidylcholines (LPCs) and lysophosphatidylethanolamines (LPEs). Chromatographic separation was achieved on an ACQUITY UPLC™ with a HSS T3 column (1.8 µm, 2.1 * 100 mm) coupled to a Q-TOF (Agilent 6530) high resolution mass spectrometer using reference mass correction. Lipids were detected in full scan in the negative ion mode. The leukotrienes, hydroxyl-fatty acids, epoxy-fatty acids and lipoxins were analysed using a fully targeted method as as previously described [52]. Oxylipid enrichment was achieved using a hydrophilic-lipophilic balance (HLB) SPE cartridge (Oasis). Oxylipid analysis used high-performance liquid chromatography (Agilent 1260) coupled to a triple-quadrupole mass spectrometer (Agilent 6460), using an Ascentis® Express column (2.7 µm, 2.1 × 150 mm).

A heatmap was generated with the software R (R Core Team (2017). R: A language and environment for statistical computing. R Foundation for Statistical Computing, Vienna, Austria.). To this end, the add-on package ggplo2 (v2.1.0) was used to run its heat map 2.0 function.

Suppression assay

Treg cells were isolated and co-cultured in complete RPMI with splenocytes labeled with 5 µM CellTrace Violet. The cells were stimulated with anti-CD3e (1µg/mL; Ebioscience), anti-CD28 (0,5µg/mL; Ebioscience) and 100U/mL recombinant mIL-2 (Peprotech). The suppressive capacity of Treg cells was determined by flow cytometry by measuring the proliferation of CellTrace Violet labeled $CD4^+$ T effector cells after 72 hours in different Treg:splenocyte ratios in which the amount of splenocytes per well were set at 50,000 cells.

Statistical analysis

Data are expressed as mean ± SD. A two-tailed student's T-test was used to compare individual groups with Gaussian distributed data. Correction for multiple comparisons was performed using Bonferroni correction. Non-parametric data was analyzed using a Mann-Whitney U-test. Data from three groups were analyzed using a one-way ANOVA with a subsequent Tukey's multiple comparison test. A p-value below 0.05 was considered significant. In the figures * indicates $p<0.05$, ** indicates $p<0.01$, *** indicates $p<0.001$ and **** indicates $p<0.0001$.

RESULTS

Diet-induced dyslipidemia decreases Treg cell homing to lymph nodes through intrinsic changes in mTORC2 signaling

Germline mutations in the *Ldlr* gene are a frequent cause of familial hypercholesterolemia and premature cardiovascular disease [20] which makes the low density lipoprotein-receptor knock-out (*Ldlr*$^{-/-}$) mouse a commonly used model to study atherosclerosis. To study alterations in Treg cell metabolism and migration in the context of dyslipidemia-induced atherosclerosis, normal chow diet (NCD) fed *Ldlr*$^{-/-}$ mice were compared to *Ldlr*$^{-/-}$ mice which were fed a Western-type diet (WTD) containing 0.25% cholesterol and 15% cocoa butter for 16-20 weeks. In this setup, WTD-fed mice develop advanced atherosclerotic lesions with a low abundance of Treg cells [4] and metabolic dysregulation in the form of hypercholesterolemia (fig. S1A) and hypertriglyceridemia (fig. S1B) but not hyperglycemia (fig. S1C).

During inflammation, Treg cells exert part of their immunosuppressive function in draining LNs of inflammatory sites [21] to which they migrate through the high-endothelial venules or lymphatic system. Since obesity-induced metabolic stress affects the migration of $CD4^+$ T cells towards LNs, we examined whether WTD-induced dyslipidemia induces intrinsic changes in Treg cells which affects their migration via a similar mechanism. We examined the splenic Treg cell population since prolonged diet-induced dyslipidemia is associated with changes in the expression of certain selectins in Treg cells, one of which is a decrease in CD62L expression (in this population) [4].

First, the number of splenic Treg cells to migrate towards the mesenteric LN in a peritoneal homing experiment was assessed. Isolated $CD4^+$ T cells from NCD- or WTD-fed donor *Ldlr*$^{-/-}$ mice were injected into CD45.1 acceptor mice and in both groups, the number of donor-derived Treg cells in the mesenteric LNs was quantified. Treg cells derived from WTD-fed mice (WTD-Treg cells) migrated less efficiently towards mesenteric LNs compared to Treg cells from NCD-fed mice (NCD-Treg cells) as the number of retrieved WTD-Treg cells was lower as compared to NCD-Treg cells (fig. 1A). During obesity-induced metabolic stress, altered PI3K activity leads to increased Akt phosphorylation at serine 473, an amino acid residue on Akt which is targeted by mTORC2. We postulated that the observed decrease in LN homing was caused by WTD-induced metabolic stress in Treg cells which increased mTORC2 activity. Through phosphorylation of Akt kinase at the serine 473 residue and subsequent phosphorylation of forkhead Box O1 (Foxo1), increased mTORC2 activity would ultimately cause decreased expression of *Klf2, CD62L*, *CCR7* and *S1pr1* in WTD-Treg cells (fig. 1B). *Klf2* is the gene encoding Krüppel-like factor 2 which, like Foxo1, is a transcription factor whose target genes include proteins that are crucial for T cells to home towards LNs, including CD62L, CCR7 and sphingosine-1-phosphate receptor 1 (S1Pr1) [22]. p-Akt S473 levels as measured by flow cytometry were confirmed to be elevated in WTD-Treg cells as compared to NCD-Treg cells (fig. 1C). Accordingly, p-Foxo1 levels as measured by immunoblot analysis were elevated as well (fig. 1D) indicating less transcriptionally active Foxo-1. In addition, *Klf2* expression was slightly decreased (fig. 1E) which, together with less functional Foxo1, resulted in decreased expression of *CD62L*, *Ccr7* and *S1pr1* (fig. 1F). This also resulted in decreased protein levels of CD62L and CCR7 (fig. 1G) as measured by flow cytometry and a decreased percentage of Treg cells expressing CD62L and/or CCR7 (fig. 1H). The percentage of $CD62L^+$ Treg cells in the circulation was also lower during dyslipidemia which, although CCR7 expression was unchanged (fig. 1I), indicates that metabolic stress in Treg cells in the spleen affects the migratory phenotype of Treg cells which egress there from and reenter the circulation.

Overall, these data indicate that, similar to diet-induced obesity, WTD-induced dyslipidemia caused intrinsic changes in mTORC2 activity in Treg cells which ultimately decreased the capacity of Treg cells to migrate towards lymph nodes.

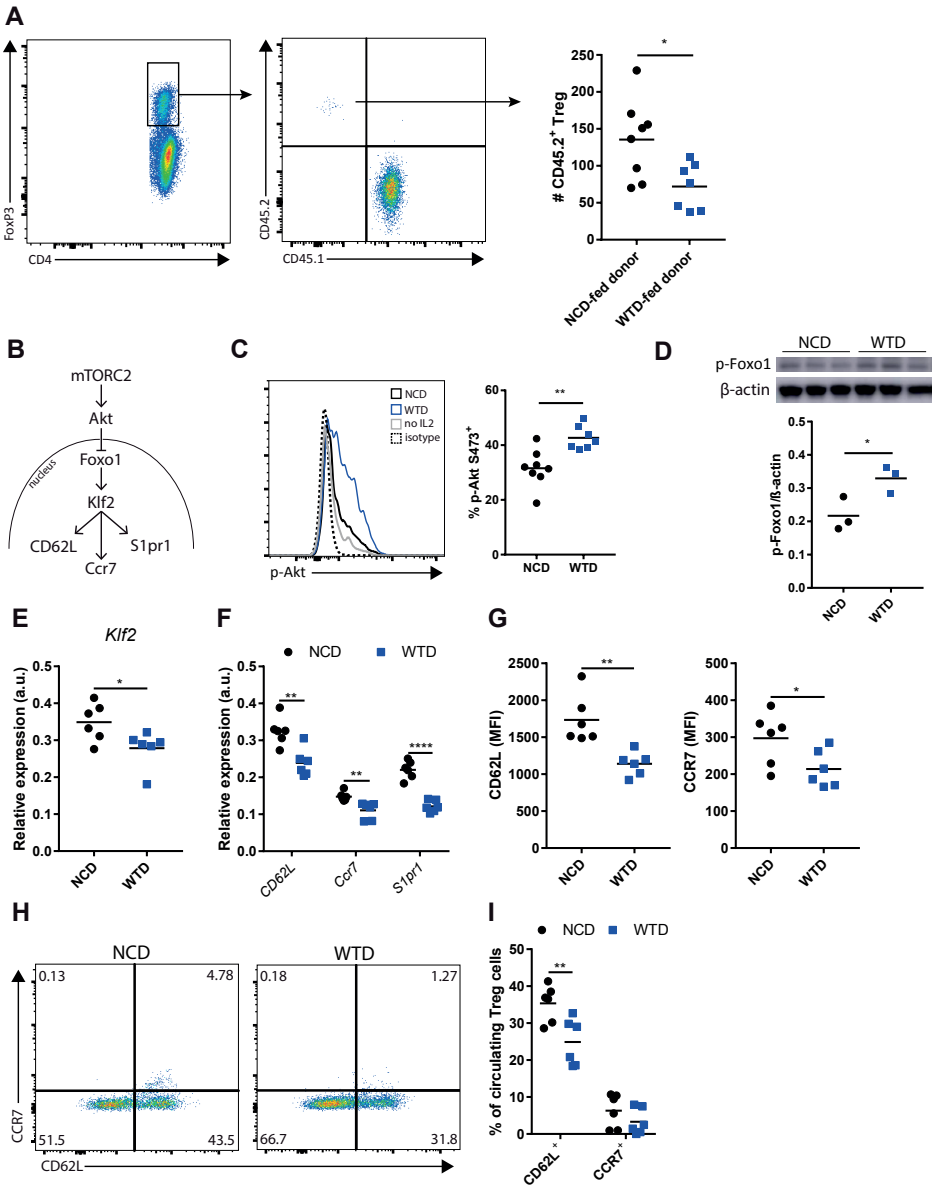

Figure 1 Diet-induced dyslipidemia in *Ldlr*$^{-/-}$ is associated with intrinsic changes in mTORC2 activity and lymph node homing of Treg cells (A) Gating strategy to identify adoptively transferred Treg cells derived from normal chow diet (NCD) or Western-type diet (WTD) fed *Ldlr*$^{-/-}$ mice which had migrated to mesenteric LN in a peritoneal homing experiment. (B) mTORC2-Akt-Foxo1-Klf2 axis. (C) p-Akt levels in splenic Treg cells derived from NCD-fed mice (NCD-Treg cells) or WTD-fed mice (WTD-Treg cells). (D) Representative data for p-Foxo1 levels in NCD- and WTD-Treg cells. (E) *Klf2* expression in NCD- and WTD-Treg cells. (F) Expression of *CD62L*, *Ccr7* and *S1pr1* in NCD- and WTD-Treg cells. (G) MFI for CD62L and CCR7 in NCD- and WTD-Treg cells. (H) representative plots of percentages of CD62L^{+} and CCR7^{+} in NCD- and WTD-Treg cells. (I) CD62L and CCR7 expression in Treg cells in the blood of NCD- and WTD-fed mice. A represents one experiment. C-H are representative data for two independent experiments. *p<0.05, **p<0.01, ***p<0.001, ****p<0.0001. MFI = median fluorescence intensity

Diet-induced dyslipidemia increses lipids and inhibits mTORC1 activity and cholesterol synthesis in Treg cells

As diet-induced dyslipidemia caused metabolic stress in splenic Treg cells, which skewed their migration, we further characterized lipid accumulation of Treg cells in other SLOs and the circulation. Diet-induced dyslipidemia potentially affects the intracellular lipids of Treg cells in various SLOs. Lipoproteins in the blood can infiltrate LNs through the high-endothelial venules or the lymphatics system and can actually enter the spleen more easily as the spleen is a very well-vascularized SLO organ.

First, we examined if cholesterol accumulation in Treg cells in the blood, spleen, draining LN and non-draining LNs is equally affected when comparing WTD-fed *Ldlr*$^{-/-}$ mice to age-matched NCD-fed control mice. The mediastinal LN (medLN) drains atherosclerotic lesions in the proximal part of the aorta while the inguinal LN (iLN) drains hind limbs which do not develop diet-induced atherosclerosis in this experimental setup. After 16 weeks of WTD, Treg cells in the spleen and mediastinal LN (medLN) showed elevated cholesterol accumulation whereas Treg cells in the blood and inguinal LN (iLN) were unaffected (fig. 2A). Next, we measured the amount of Treg cells in these organs and observed an increase in Treg cells specifically in the spleen and medLN (fig. 2B). In the spleen, this increase in the percentage of Treg cells resulted in a strongly expanded splenic Treg cell population (fig. 2C). A lipid droplet staining showed that besides cholesterol accumulation in Treg cells, dyslipidemia was also associated with lipid droplet accumulation in Treg cells in the spleen and medLN (fig. 2D). These findings are especially relevant as splenic Treg cells encounter blood-borne antigens (e.g. derived from modified LDL [23]). Accordingly, antigen-specific Treg cells can be found in the spleen during atherosclerosis [24]. Presumably, the increase in Treg cells and their lipid content in the medLN is due to ongoing inflammation in atherosclerotic lesions which contains copious amounts of (modified) lipoproteins which are drained to the medLN .

Interestingly, the level of cholesterol which accumulated in WTD-Treg cells was sufficient to decrease mTORC1 activity as compared to NCD-Treg cells (fig. 2E). The decrease in mTORC1 activity was confirmed by measuring phospho-S6 levels in isolated Treg cells using immunoblot analysis (fig. 2F). In addition, the expression of *Srebp1* and *Srebp2*, whose expression is decreased by inhibition of mTORC1 [25,26], was diminished in WTD-Treg cells (fig. S1D). Concomitantly, the expression of enzymes which are crucially involved in cholesterol synthesis through the mevalonate pathway was decreased, particularly that of *Hmgcs1, Idi1* and *Fdft1,* whose expression was decreased by approximately 50% (fig. 2G). Treg cells which lack Raptor, an essential protein in mTORC1, lose their suppressive capacity which is mostly due to reduced activity of the mevalonate pathway in proliferating Treg cells [8]. As compared to NCD-Treg cells, WTD-Treg cells had similar suppressive function as measured by their capacity to suppress proliferation of $CD4^+$ T effector cells (Fig. S1E). mTORC1 activity as measured by p-S6 levels was also decreased

in $CD4^+FoxP3^-$ conventional T (Tconv) cells from WTD-fed mice (fig. S1F) which indicates diet-induced dyslipidemia also exerts metabolic stress on non-Treg cells.
To confirm that the observed changes were specifically caused by dyslipidemia, we mimicked it *in vitro* by culturing Treg cells in culture medium supplemented with serum from NCD or WTD-fed mice (fig. 2H) or supplemented with isolated β-very low density lipoprotein (β-VLDL) particles. Lipid loading *in vitro* through serum supplementation mimicked the effects of hypercholesterolemia on mTORC1 activity as measured by p-S6 and p-4E-BP1 (an additional mTORC1 target) levels in Treg cells (fig. 2I). Moreover, this effect of serum supplementation also occurred in Treg cells isolated from C57/BL6 mice and additional treatment of Treg cells with the mTOR inhibitor rapamycin severely diminished the WTD-serum induced inhibition of mTORC1 (fig. 2J). Additionally, the p-S6 levels were reduced by approximately 50% when incubating Treg cells with isolated β-VLDL particles as compared to the vehicle control (fig. 2K).
Altogether, these results showed that diet-induced dyslipidemia induced lipid accumulation in Treg cells, which reduced mTORC1 activity and the expression of genes crucially involved in the mevalonate pathway without altering their suppressive capacity.

WTD-Treg cells have impaired glycolysis but increased FA oxidation

Next, we reasoned that dyslipidemia-induced mTORC1 inhibition would change the bioenergetic metabolism in Treg cells. mTOR kinase is a crucial regulator of energetic metabolism which can regulate glycolysis by increasing the transcription and translation of HIF1α [26,27]. We measured glycolysis in NCD-Tregs and WTD-Tregs using an XF analyzer (fig. 3A) and observed a small decrease in basal extracellular acidification rate (ECAR), which is a measure for lactate producing glycolysis. Furthermore, when compared to NCD-Treg cells, WTD-Treg cells had decreased glycolytic reserve and glycolytic capacity upon exposure of Treg cells to the complex I inhibitor oligomycin (Fig. 3B). As we observed a decrease in mRNA expression of the target genes of HIF1α (*Glut1, Pgk1, LDHa, Pkm2*) when culturing Treg cells with WTD serum in vitro (fig. S2A) we speculated that WTD-induced dyslipidemia decreased HIF1α expression in Treg cells, thereby decreasing glycolysis. However, immunoblot analysis revealed that HIF1α levels were unchanged (Fig. S2B) as were the mRNA expression levels of *Glut1, Pgk1, LDHa, Pkm2* (fig. S2C) in freshly isolated WTD-Treg cells as compared to NCD-Treg cells. Similar to HIF1α, through signaling down-stream of mTORC1, Myc can transcriptionally regulate the expression of glycolytic genes [16]. Myc expression was also equal between NCD-Treg and WTD-Treg cells (fig. S2D). As the Treg cells in which we measured glycolysis were activated with anti-CD3/CD28 and IL-2 prior to the measurements it is likely that mTORC1 inhibition by excess intracellular cholesterol only affected the expression of downstream target genes of HIF1α or Myc upon activation as mTORC1 activity is increased upon activation[8]. mTORC1 activation also promotes mitochondrial biogenesis [28]. The mitochondrial mass

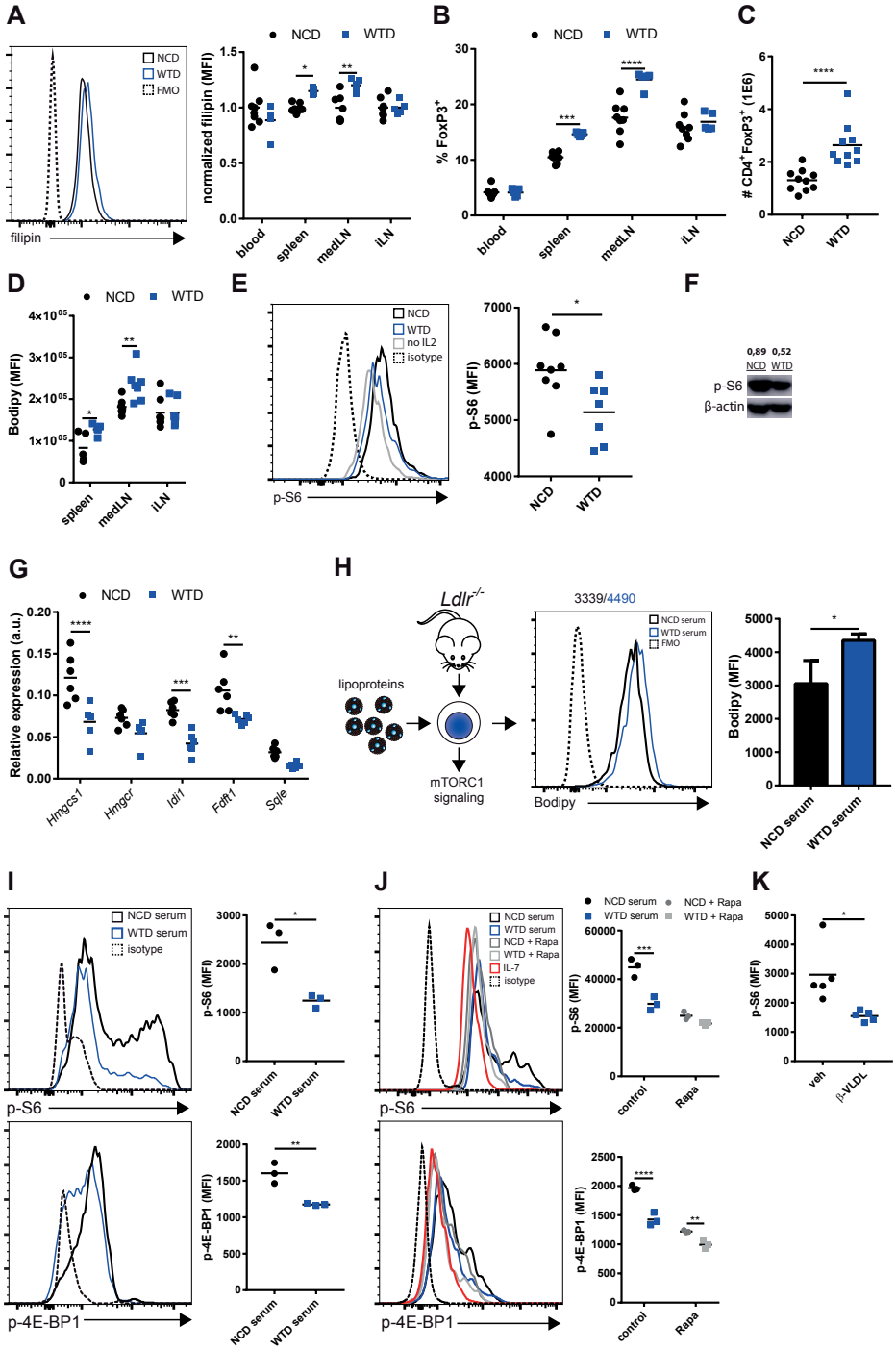
A
NCD
WTD
FMO
filipin
normalized filipin (MFI)
blood
spleen
medLN
iLN
B
% FoxP3+
C
CD4+FoxP3+ (1E6)
D
Bodipy (MFI)
E
no IL2
isotype
p-S6
p-S6 (MFI)
F
0,89
0,52
p-S6
β-actin
G
Relative expression (a.u.)
Hmgcs1
Hmgcr
Idi1
Fdft1
Sqle
H
Ldlr-/-
lipoproteins
mTORC1 signaling
3339/4490
NCD serum
WTD serum
FMO
Bodipy
Bodipy (MFI)
I
isotype
p-S6
p-4E-BP1
p-4E-BP1 (MFI)
J
NCD + Rapa
WTD + Rapa
IL-7
control
Rapa
K
veh
β-VLDL

Figure 2 mTORC1 activity is diminished in Treg cells from WTD-fed *Ldlr*$^{-/-}$ mice. (A) Filipin staining for cholesterol in Treg cells from blood, spleen, mediastinal lymph node (medLN) and inguinal lymph node (iLN). (B) Percentage of Treg cells in same tissues as in (A). (C) Number of Treg cells in spleen. (D) Bodipy staining for lipid droplets in Treg cells. (E) p-S6 levels as measured by flow cytometry (F) p-S6 level in isolated splenic Treg cells using immunoblot. p-S6 levels as assessed by immunoblot were normalized for β-actin levels as shown above the lanes. (G) Expression of genes from mevalonate pathway in isolated Treg cells (H) *In vitro* lipid loading of Treg cells to study mTORC1 signaling (I) p-S6 and p-4E-BP1 levels after 48h *in vitro* lipid loading with serum. (J) p-S6 and p-4E-BP1 levels after 48h *in vitro* lipid loading of wildtype Treg cells with rapamycin and/or serum. Interleukin-7 (IL-7) was used to sustain Treg cells without anti-CD3 stimulation. (H) p-S6 levels after lipid loading with β-VLDL. A-E and G-I are representative data for 3 individual experiments. J represents 1 experiment. K is representative for 2 individual experiments. MFI = median fluorescence intensity. FMO = fluorescence minus one control. *p<0.05, **p<0.01, ***p<0.001, ****p<0.0001. The data in H represents the mean±standard deviation.

in Treg cells was equal in both groups (fig. 3C) and when measuring oxygen consumption rate (OCR) as a measure for oxidative phosphorylation, we observed no differences between NCD-Treg cells and WTD-Treg cells (fig. 3D), which implicated that diet-induced dyslipidemia did not induce changes in mitochondrial function.

As mTORC1 can also regulate FA oxidation through inhibition of the rate-limiting enzyme carnitine palmitoyltransferase 1 (CPT1), we measured the detritiation of ^{3}H-palmitic acid as a measure for FA oxidation. Pharmacological mTOR inhibition *in vitro* with rapamycin increased the rate of mitochondrial FA oxidation (calculated by subtracting the detritiation of ^{3}H-palmitic acid with etomoxir from the total ^{3}H-palmitic acid detritiation) with or without etomoxir in Treg cells as compared to the control (fig S2E). In line with dyslipidemia-induced mTORC1 inhibition, Treg cells from WTD fed mice showed about twice the level of mitochondrial FA oxidation (fig. 3E) and a comparable increase in *Cpt1a* expression (fig. 3F). FA oxidation in Tconv cells was unaffected by diet-induced dyslipidemia, suggesting that metabolic modulation by dyslipidemia were Treg cell-specific (fig. S2F). Mitochondrial FA oxidation has been shown to be crucial for Treg cell proliferation [9] although it must be noted that CPT1 deficient Treg cells proliferate normally [29]. We compared the proliferation of WTD-Treg cells to NCD-Treg cells by measuring the percentage of Ki-67^{+} Treg cells but this was unaltered (fig. S2G). To examine whether the metabolic adaptations in WTD-Treg cells were induced by diet-induced dyslipidemia and not by the chronic low-grade inflammation which is associated with atherosclerosis [30], we performed a diet-switch experiment in which we reverted WTD-fed mice to an NCD. Ten weeks after reverting WTD-fed mice to an NCD, atherosclerotic plaque size is similar as compared to prior to the diet-switch [31,32]. Thus, a diet-switch normalizes the circulating lipid levels without decreasing the degree of atherosclerosis, thereby uncoupling the contribution of circulating lipids from atherosclerosis-associated low-grade inflammation in the effect that diet-induced dyslipidemia has on FA metabolism in Treg cells 18 days after reverting the mice to an NCD, total cholesterol levels in the serum were

normalized in the DS group (fig. 3G). Accordingly, cholesterol levels were normalized in Treg cells from diet-switch mice (hereafter referred to as DS-Treg cells) (fig. 3H). Gene expression of liver-X-receptor (which is activated by cholesterol-derivatives) target genes *Abca1* and *Abcg1* were increased in WTD-Treg cells but not in DS-Treg cells (fig. 3I), confirming that the cholesterol levels in Treg cells were normalized by a diet-switch. Counterintuitively, flow cytometric analysis revealed that mTORC1 activity in DS-Treg cells was diminished as compared to NCD-Treg cells, suggesting that normalization of mTORC1 activity might occur gradually after normalization of cellular cholesterol levels (fig. 3I). Strikingly, despite mTORC1 activity being attenuated, mitochondrial FA oxidation in DS-Treg cells did not differ significantly from NCD-Treg cells, and *Cpt1a* expression was also equal between these groups (fig. 3J).
Collectively, these data indicate that glycolysis and FA oxidation are modulated by dietary lipids during dyslipidemia but that the latter effect of dyslipidemia is not exclusively mediated by mTORC1.

WTD increases PPARδ ligands in serum and increases the expression of PPARδ target genes

As we observed that a decrease in mTORC1 activity alone was not sufficient to increase mitochondrial FA oxidation we sought to determine which additional mechanism(s) could be responsible. Since FA oxidation in Treg cells was affected by the composition of the diet, we reasoned that peroxisome proliferator activated receptors (PPAR) were involved as these nuclear receptors are activated by dietary lipids and can modulate cellular metabolism.
The PPAR proteins, PPARα -δ and –γ, have limited overlap in their natural ligands and biological function [33,34]. We were unable to detect *PPARα* expression in NCD- or WTD-Treg cells (fig. S4A). PPARδ and PPARγ share some of their target genes. Since PPARγ target genes are involved in the uptake and biosynthesis of lipids and *PPARδ* expression was about 10-fold higher compared to *PPARγ* expression in Treg cells (Fig. S3A), it seemed plausible that any PPAR-mediated effects were mainly PPARδ mediated. In support of this, the mRNA expression of PPARγ target genes *Scd1* and *Dgat* was unaltered between NCD- and WTD-Treg cells (fig. S3B).
In skeletal muscle, PPARδ activation using a synthetic ligand increases FA oxidation by increasing the expression of genes involved in FA catabolism (including *Cpt1*) and reduces glucose catabolism by reducing the expression of genes involved in glycolysis [35]. To examine whether diet-induced dyslipidemia activated PPARδ in our study we first treated isolated Treg cells with GW501516, a PPARδ agonist, *in vitro.* GW501516 treatment increased the expression of *Cpt1a, Slc25a20* and *Plin2* while decreasing *Lipe* expression (fig. 4A). *Slc25a20* and *Plin2* expression were increased and *Lipe* expression was decreased in WTD-Treg cells as compared to NCD-Treg cells (fig. 4B), indicating that

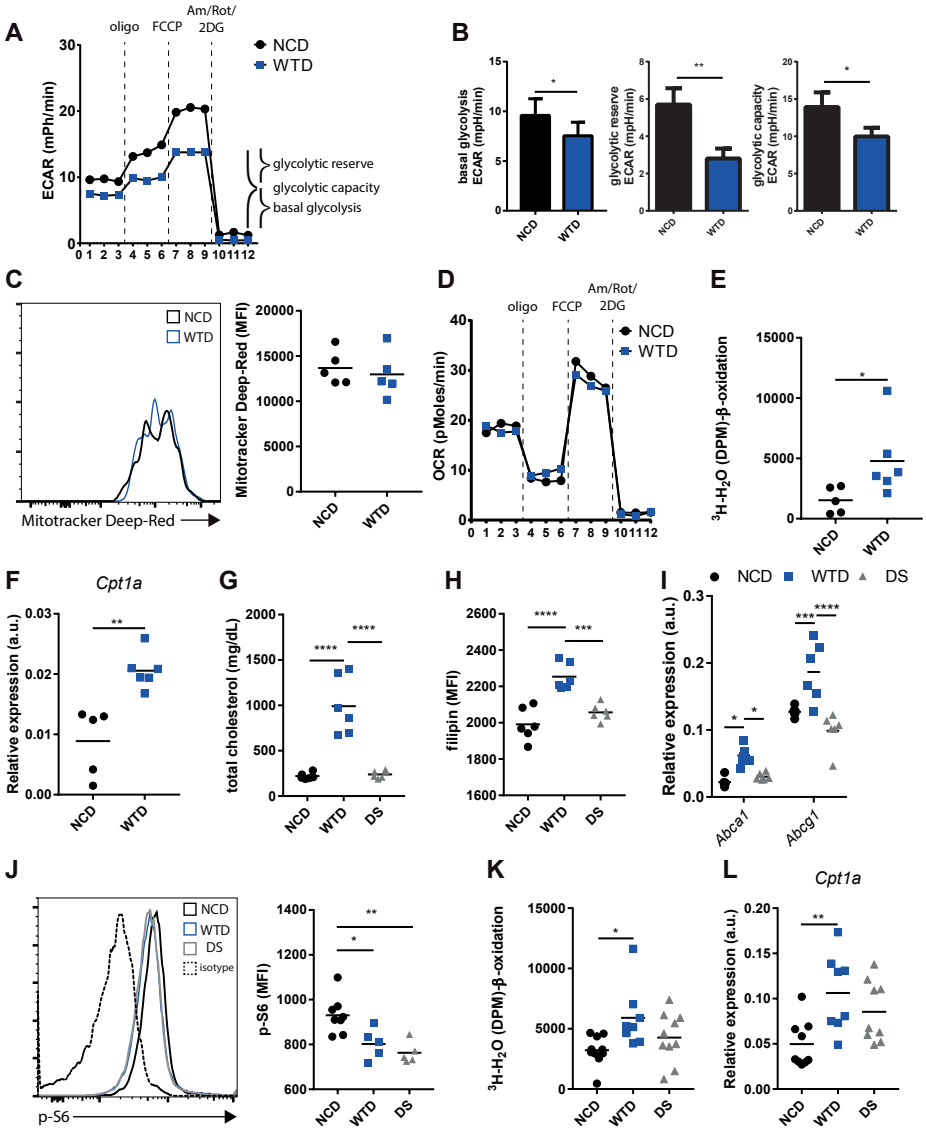

Figure 3. Diet-induced dyslipidemia in *Ldlr*$^{-/-}$ mice impaired glycolytic metabolism but enhanced mitochondrial FA metabolism in WTD-Treg cells. (A) Extracellular acidification rate (ECAR) during of NCD-Tregs and WTD-Tregs in response to oligomycin (oligo), carbonyl cyanide-4-(trifluoromethoxy)phenylhydrazone (FCCP), antimycin-A (Ant), rotenone (Rot) and 2-deoxyglucose (2-DG). (B) Basal glycolysis, glycolytic reserve and glycolytic capacity quantified from (A). (C) Mitochondrial mass in Treg cells (D) Oxygen consumption rate (OCR) in same assay as in (A). (E) ^{3}H-palmitic acid detritiation in isolated Treg cells from indicated groups (F) *Cpt1a* expression in isolated Treg cells. (G) Total serum cholesterol levels from diet-switch experiment (H) Cellular cholesterol staining in Treg cells (I) Expression of cholesterol efflux transporters *Abca1* and *Abcg1*. (J) p-S6 levels as measured by flow cytometry (K) ^{3}H-palmitic acid detritiation after 4h incubation with ^{3}H-palmitic acid (L) *Cpt1a* expression in diet switch experiments. A,-J represents data from 2 independent experiments. Data in K and L is pooled from two independent experiments showing similar effects. DS = diet switch group *p<0.05, **p<0.01, ***p<0.001, ****p<0.0001. The data in B represents the mean±standard deviation.

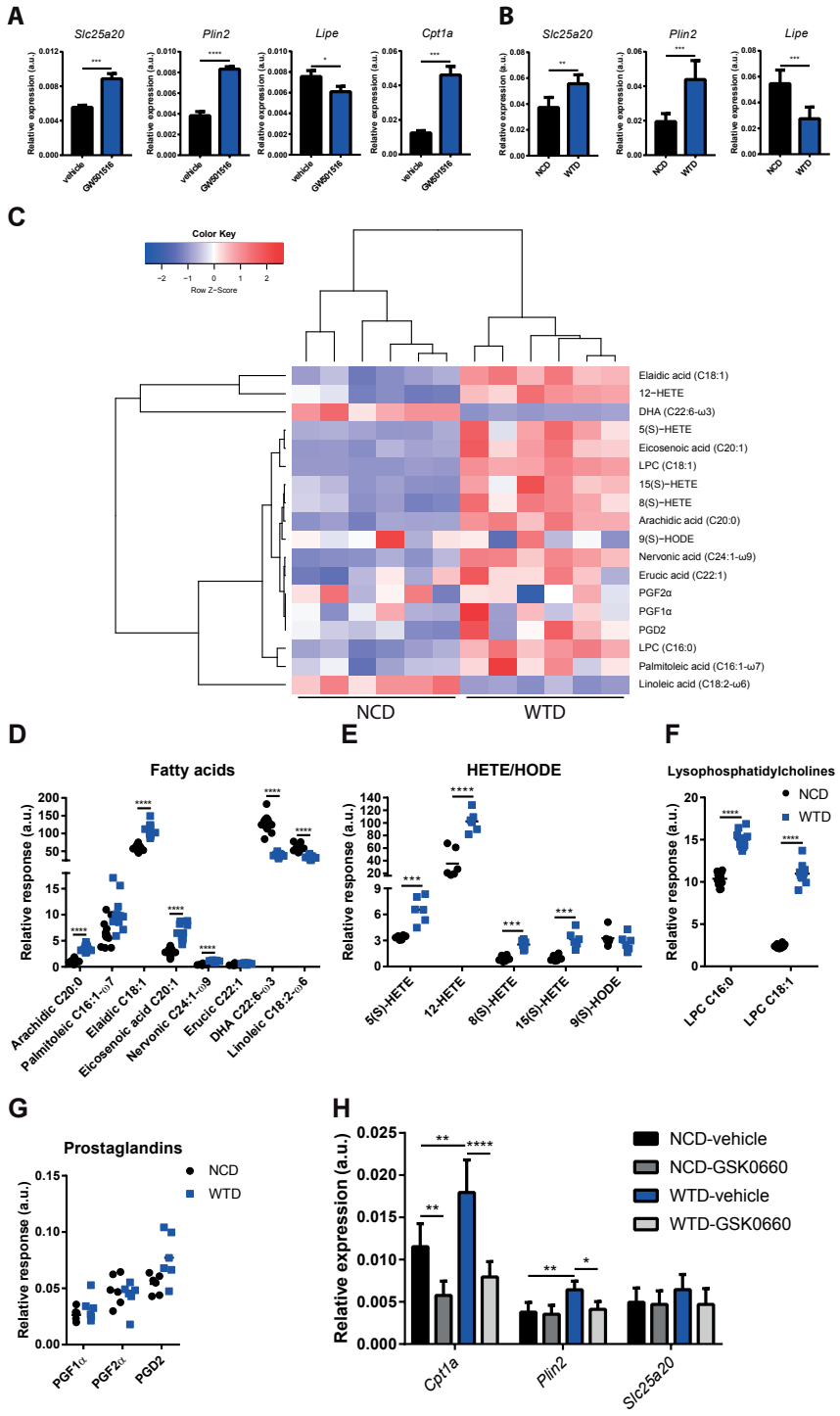
A
Slc25a20
Plin2
Lipe
Cpt1a
Relative expression (a.u.)
vehicle
GW501516
B
Slc25a20
Plin2
Lipe
NCD
WTD
C
Color Key
Row Z-Score
Elaidic acid (C18:1)
12−HETE
DHA (C22:6-ω3)
5(S)−HETE
Eicosenoic acid (C20:1)
LPC (C18:1)
15(S)−HETE
8(S)−HETE
Arachidic acid (C20:0)
9(S)−HODE
Nervonic acid (C24:1-ω9)
Erucic acid (C22:1)
PGF2α
PGF1α
PGD2
LPC (C16:0)
Palmitoleic acid (C16:1-ω7)
Linoleic acid (C18:2-ω6)
NCD
WTD
D
Fatty acids
Relative response (a.u.)
Arachidic C20:0
Palmitoleic C16:1-ω7
Elaidic C18:1
Eicosenoic acid C20:1
Nervonic C24:1-ω9
Erucic C22:1
DHA C22:6-ω3
Linoleic C18:2-ω6
E
HETE/HODE
Relative response (a.u.)
5(S)-HETE
12-HETE
8(S)-HETE
15(S)-HETE
9(S)-HODE
F
Lysophosphatidylcholines
NCD
WTD
Relative response (a.u.)
LPC C16:0
LPC C18:1
G
Prostaglandins
NCD
WTD
Relative response (a.u.)
PGF1α
PGF2α
PGD2
H
Relative expression (a.u.)
NCD-vehicle
NCD-GSK0660
WTD-vehicle
WTD-GSK0660
Cpt1a
Plin2
Slc25a20

Figure 4 Diet-induced dyslipidemia in *Ldlr*$^{-/-}$ mice increases circulating PPARδ ligands and elevates PPARδ target gene expression in Treg cells (A) Expression of PPARδ target genes in Treg cells treated with GW501516 or vehicle *in vitro* (B) Expression of same genes as in (A) minus *Cpt1a* in NCD- and WTD-Treg cells (C) Heatmap of natural PPARδ ligands in serum from NCD and WTD-fed mice. (D) Relative abundance of PPARδ ligands from fatty acids subclass. (E) Relative abundance of PPARδ ligands from hydroxyeicosatetraenoic acid (HETE) and hydroxyoctadecadienoic acid (HODE) subclasses (F) Relative abundance of PPARδ ligands from lysophosphatidylcholine subclass. (G) Relative abundance of PPARδ ligands from prostaglandin subclass. (H) Expression of PPARδ target genes after *in vitro* treatment with GSK0660 or vehicle (DMSO) treatment. *<0.05, **p<0.01, ***p<0.001, ****<p<0.000. The data in A, B and H represent the mean±standard deviation.

specific target genes of PPARδ which are involved in FA catabolism (*Slc25a20*, *Lipe*) and lipid droplet formation (*Plin2*) are modulated by dyslipidemia.

CD36 is a scavenger receptor involved in the uptake of FAs and (modified) lipoproteins. It is a transcriptional target of PPARγ [36] and CD36-mediated uptake of FAs can modulate the activity of PPARδ whose target genes are involved in FA- and glucose metabolism [37]. Compared to NCD-Treg cells, CD36 expression was increased in WTD-Treg cells but not in DS-Treg cells (fig. S3C), suggesting that elevated CD36 expression might contribute to the increased mitochondrial FA oxidation in WTD-Treg cells by increasing the uptake of lipids. CD36 expression in Tconv cells from WTD-fed mice was also increased but remained far lower as compared to Treg cells (fig. S3D), possibly explaining why the latter are more sensitive to perturbations in environmental lipid levels.

To confirm WTD-induced dyslipidemia increased the levels of circulating PPARδ ligands, we performed metabolomics profiling by high-performance liquid chromatography and mass spectrometry of the free and total oxidized lipids in sera of NCD- and WTD fed mice. We selected previously described PPARδ ligands [38–40] which were included in our lipidomics platform and examined relative increases or decreases in the abundance of these lipids. In general, PPARδ ligands were increased in sera of mice which were fed a WTD compared to NCD fed *Ldlr*$^{-/-}$ mice (Fig. 4C). Of the eighteen PPARδ ligands we examined, only two were less abundant in sera of WTD fed mice while eleven were more abundant. Especially lipids from the saturated- and monounsaturated FAs (fig. 4D) , hydroxyeicosatetraenoic acid (HETE) (fig. 4E) and lysophosphatidylcholine (fig. 4F) subclasses were relatively increased after 8 weeks of WTD as compared to NCD. There were no changes in the abundance of serum prostaglandins (fig. 4G). HETEs can be synthesized from various polyunsaturated FAs, including arachidonic acid (AA), dihomo-γ-linolenic acid (DGLA) or eicosapentaenoic acid (EPA) through similar pathways. AA (20:4 ω-6) showed a small relative decrease in WTD serum as compared to NCD serum (fig S3E). Relative EPA abundance was decreased as well (fig. S3F) but DGLA (fig. S3G) was increased, suggesting that an increase of DGLA in the serum contributed to increased HETE synthesis and circulating HETEs. Specific triglyceride-derived FAs, which were identified as potent natural ligands for PPARδ but not for PPARγ in macrophages [38], were

increased during WTD-induced dyslipidemia, including palmitoleic, elaidic, eicosenoic, and erucic acid. Reverting the WTD group to an NCD normalized the free fatty acid levels (FFA) in the serum (Fig. S3H) as well as serum triglycerides (fig. S3I). Lastly, we treated isolated Treg cells *in vitro* with the PPARδ antagonist/inverse agonist GSK0660 to confirm that the increase in *Cpt1a*, *Plin2* and *Slc25a20* was PPARδ-mediated. The increased expression in *Cpt1a* and *Plin2* but not of *Slc25a20* in WTD-Treg cells was sensitive to a 4h treatment with GSK0660 *in vitro* (fig. 4H) suggesting that PPARδ was indeed activated by WTD-induced dyslipidemia but that pharmacological inhibition of PPARδ activity did not abolish this entirely.

The presented data show that dyslipidemia increased the abundance of PPARδ ligands in the circulation, thereby increasing PPARδ activity in Treg cells and contributing to alterations in their bioenergetic metabolism.

Treg cells with high rates of FA oxidation migrate more efficiently towards sites of inflammation

Since PPARδ contributed to metabolic adaptations in WTD-Treg cells and we hypothesized that the changes in glycolytic and FA metabolism could affect their migration, we mimicked that effect of dyslipidemia by treating purified Treg cells *in vitro* with the PPARδ agonist GW501516 and assessed Treg cell migration. Similar to WTD-Treg cells, mitochondrial FA oxidation was increased in GW501516-treated Treg cells (fig. 5A). Additionally, GW501516 treatment decreased Glut1 expression on Treg cells on an mRNA (fig. 5B) and protein level (fig. 5C) without affecting the expression of membrane proteins involved in migration, including CCR5, CCR7, CXCR3, CD62L and LFA-1 (fig. S4A). A peritoneal homing experiment showed that GW501516-treated Treg cells migrated more efficiently towards the inflamed peritoneum as compared to vehicle control (fig. 5D). Moreover, this effect was FA oxidation-dependent as pre-incubating GW501516-treated Treg cells with a 100 μM of the irreversible CPT1 inhibitor etomoxir abolished their enhanced migratory capacity. A 100 μM etomoxir concentration is relatively high, but has no off-target effects on oxidative phosphorylation [29]. Etomoxir treatment did not affect the viability of Treg cells treated with dimethyl sulfoxide (DMSO) or GW501516 indicating the decreased number of Treg cells pre-treated with etomoxir, which we recovered from the inflamed peritoneum. was not due to increased cell death (fig. 5E). To validate these findings *in vitro*, a transwell migration assay with CCL21 was performed which confirmed that GW501516-treated Treg cells displayed more potent migration, again in an FA oxidation dependent fashion (fig. 5F). As mentioned above, Treg cells from WTD-fed *Ldlr*$^{-/-}$ mice are less capable to bind to activated endothelium as compared to Treg cells from NCD-fed *Ldlr*$^{-/-}$ mice [4]. As we unraveled a metabolic phenotype in WTD-Treg cells that may promote their migratory capacity, we assessed this in a peritoneal homing assay. Although the number of migrated WTD-Treg cells was equal compared to NCD-fed

donor derived Treg cells (fig. 5G) the percentage of WTD-Treg cells in the peritoneal Treg cell population was higher than NCD-Treg cells (fig. 5H). Supposedly, this was because the total number of Treg cells which were recruited towards the inflamed peritoneum in the WTD-Treg cell-injected mice was lower but the migratory capacity of WTD-Treg cells was higher as compared to the CD45.1^{+} acceptor Treg cells. To further examine WTD-Treg cell migration in the context of atherosclerosis, we performed an *in vitro* aorta homing experiment with NCD- and WTD-Treg cells with or without pre-incubation with etomoxir. We incubated Treg cells with isolated atherosclerotic aortas from apolipoprotein E deficient mice, which had previously developed advanced atherosclerotic lesions. Interestingly, WTD-Treg cells migrated more efficiently into atherosclerotic lesions as compared to NCD-Tregs (fig. 5I). Surprisingly, as opposed to GW501516-treated Treg cells, the increased migratory capacity of WTD-Treg cells was only mildly affected by pre-treatment with etomoxir, suggesting that despite dyslipidemia-induced skewing of bioenergetic metabolism WTD-Treg cells were sufficiently flexible to generate the required amounts of ATP using alternative fuel sources.
In conclusion, these results indicate that activation of PPARδ and FA oxidation increases Treg cell migration and that dyslipidemia does not reduce but actually promotes migration of Treg cells towards sites of inflammation.

Diet-induced dyslipidemia affects the cellular lipid content of T cells inside atherosclerotic lesions of *Ldlr*$^{-/-}$ mice

As we established that Treg cells in specific SLOs were affected by dyslipidemia-induced lipid accumulation, we next focused on Treg cells which had migrated into atherosclerotic lesions as their function is crucial for immunosuppression at the site of inflammation. Using flow cytometry, we assessed the amount of cholesterol and lipid droplets in CD4^{+}CD25^{hi} T cells from atherosclerotic lesions of the aortic arches of NCD- and WTD-fed *Ldlr*$^{-/-}$ mice (fig. 6A). In atherosclerotic aortic arches, similar to the spleen and medLN, the amount of cholesterol (fig. 6B) and lipid droplets (fig. 6C) was higher in CD4^{+}CD25^{hi} T cells from WTD-fed mice as compared to NCD-fed mice. It must be noted that it is unlikely that, as opposed to the spleen and medLN, aortic CD4^{+}CD25^{hi} T cells predominantly represent Treg cells as these can also be activated Tconv cells. We measured CD36 expression in these cells to get an indication of whether the extent of lipid-induced metabolic stress was sufficient to induce PPAR activation. Again, similar to the Treg cell populations of the spleen and medLN, WTD-induced dyslipidemia was associated with increased expression of CD36 in CD4^{+}CD25^{hi} T cells from the atherosclerotic aortic lesions as compared to NCD controls (fig. 6D).
In conclusion, the T(reg) cell population in atherosclerotic lesions from WTD-fed *Ldlr*$^{-/-}$ mice contained more cholesterol and lipid droplets as compared to NCD-fed mice which is similar to what we observed in the spleen and medLN.

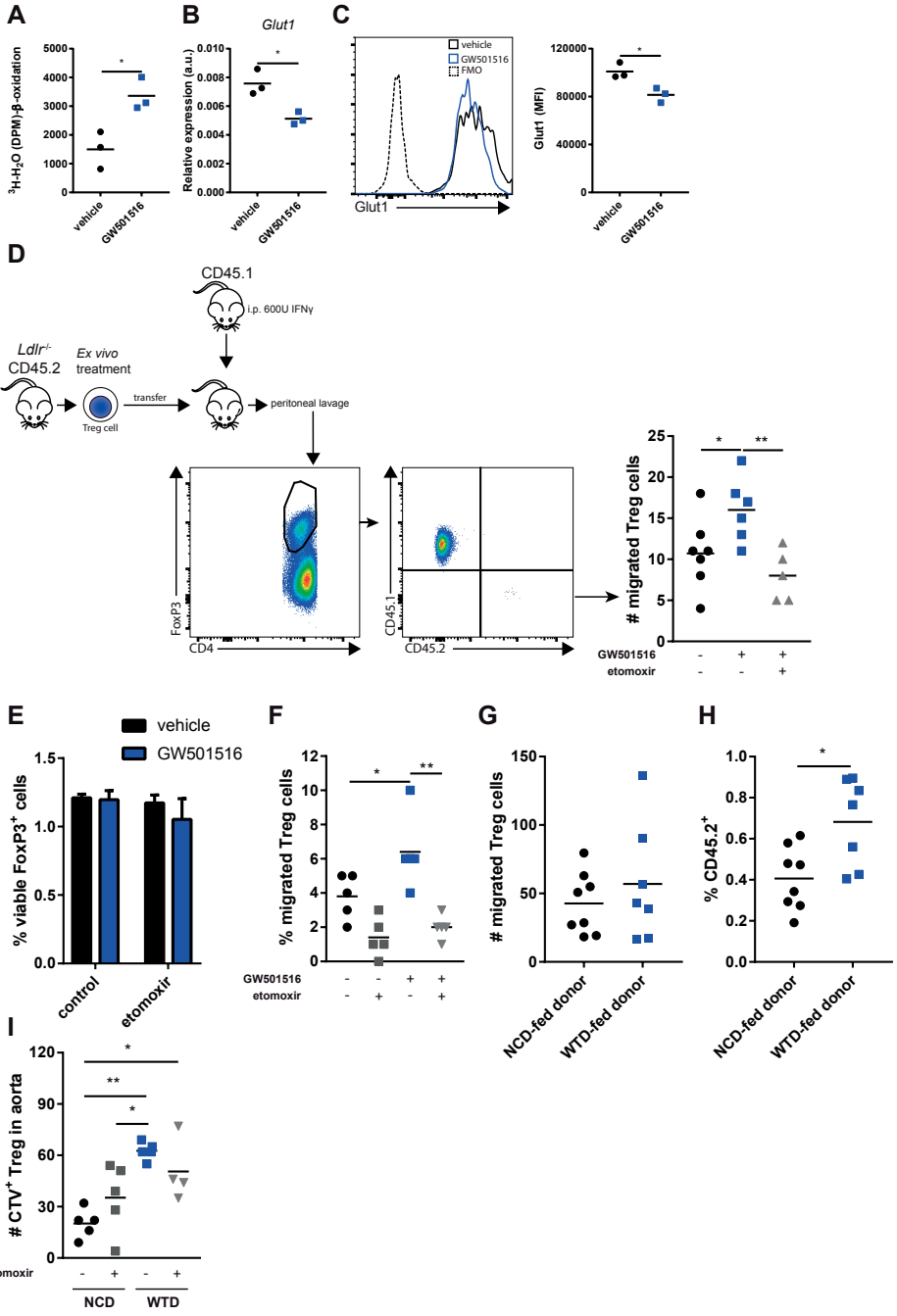
A
B
Glut1
C
vehicle
GW501516
FMO
Glut1
Glut1 (MFI)
^{3}H-H$_2$O (DPM)-β-oxidation
Relative expression (a.u.)
D
CD45.1
i.p. 600U IFNγ
Ldlr$^{-/-}$
CD45.2
Ex vivo
treatment
transfer
Treg cell
peritoneal lavage
FoxP3
CD4
CD45.1
CD45.2
migrated Treg cells
GW501516
etomoxir
E
vehicle
GW501516
% viable FoxP3$^+$ cells
control
etomoxir
F
% migrated Treg cells
G
migrated Treg cells
NCD-fed donor
WTD-fed donor
H
% CD45.2$^+$
I
CTV$^+$ Treg in aorta
NCD
WTD

Figure 5 Increased FA oxidation increases *Ldlr*$^{-/-}$ Treg cell migration (A) ^{3}H-palmitic acid detritiation in GW501516 treated Treg cells. (B) RT-qPCR analysis of *Glut1* expression. (C) Flow cytometry analysis of Glut1 expression. (D) Peritoneal homing experiment of GW501516 treated Treg cells. (E) Viability of Treg cells with indicated treatments (F) Transmigration assay towards 250ng/mL CCL21 of Treg cells treated as indicated. (G) Peritoneal homing experiment of NCD-Tregs versus WTD-Tregs. CD4^{+} T cells from NCD or WTD mice were injected i.v. and the number of Treg cells retrieved from the peritoneum were normalized for the number of Treg cells which were injected in the different CD4^{+} fractions. (H) Percentage of transferred NCD- and WTD-Treg cells relative to total number of peritoneal Treg cells (I) In vitro homing assay of NCD-Treg cells versus WTD-Treg cells with or without pre-incubation with 100 μM etomoxir. Treg cells were left to migrate towards atherosclerotic aortas from *Apoe*$^{-/-}$ mice. A-C and F represents data of 2/3 independent experiments. D represents data from 2 pooled experiments which showed similar effects. G-I represents data from one experiment. *p<0.05, **p<0.01. The data in E represents the mean±standard deviation.

DISCUSSION

A decrease in Treg cells in atherosclerotic lesions is associated with the degree of dyslipidemia. We showed that Treg cells accumulate (free) cholesterol and other neutral lipids during dyslipidemia which, through intrinsic changes in mTORC1/mTORC2 signaling and PPARδ activity, skewed their migration towards sites of inflammation instead of LNs. Pharmacological activation of PPARδ with GW501516 mimicked the effects of dyslipidemia on FA oxidation in Treg cells and increased their migration towards sites of inflammation. These findings suggest that the decrease in Treg cell immunosuppression in advanced atherosclerosis is not due to dyslipidemia-induced impairments in migratory capacity as dyslipidemia biased migration towards sites of inflammation.

An important point to address is how Treg cell-mediated immunosuppression is decreased in atherosclerotic lesions while diet-induced dyslipidemia induces intrinsic (metabolic) changes which skews their migratory phenotype, presumably in a beneficial manner. We propose that diet-induced dyslipidemia enhances the capacity of Treg cells to migrate towards sites of inflammation but that the local environment inside atherosclerotic lesions is unfavorable for Treg cells, thereby disrupting their immunosuppressive capacity. In support of this, Treg cells inside murine atherosclerotic lesions become increasingly apoptotic as lesions progress during diet-induced atherosclerosis an effect, which is counteracted by restoration of normocholesterolemia [4]. The main culprit lipoprotein in atherosclerosis is the cholesterol-rich LDL particle, which becomes oxidized in the vessel wall. Oxidized LDL (oxLDL) can dose-dependently induce apoptosis in human Treg cells [41] and has been suggested to induce apoptosis in murine Treg cells as well [7]. This suggests that dyslipidemia itself contributes to a microenvironment inside lesions which is especially unfavorable for Treg cells.

Another feasible explanation for a loss of Treg cells inside lesions, in addition to increased local apoptosis, is that Treg cells might lose expression of FoxP3 inside atherosclerotic lesions and are therefore not identifiable as Treg cells. Indeed, oxLDL can increase meth-

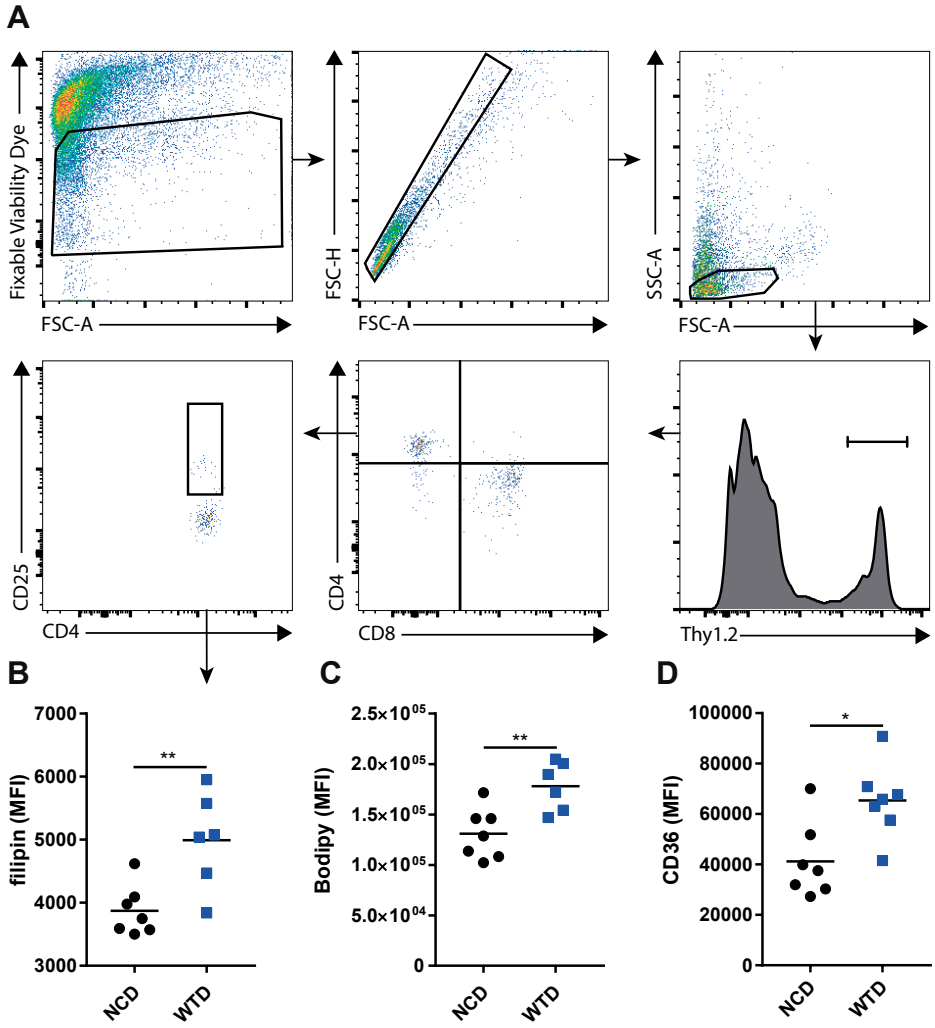

Figure 6 The effects of WTD-induced dyslipidemia on CD4^{+}CD25^{hi} T cells in atherosclerotic lesions from *Ldlr*$^{-/-}$ mice (A) The gating strategy for CD4^{+}CD25^{hi} T cells in atherosclerotic lesions from the aortic arch. (B) Filipin staining in CD4^{+}CD25^{hi} T cells. (C) Bodipy staining in CD4^{+}CD25^{hi} T cells. (D) CD36 staining in CD4^{+}CD25^{hi} T cells. *<0.05, **p<0.01.

ylation of the demethylated regions in the promotor of the *FoxP3* gene in Treg cells from healthy subjects [42], resulting in decreases of *FoxP3* expression in Treg cells. Also in the microenvironment of murine atherosclerotic lesions, a CD4^{+} T cell population expressing both FoxP3 and Tbet has been described [43] although it is unclear whether these cells originated from Treg cells. Moreover, WTD-induced atherogenesis was recently shown

to decrease FoxP3 expression in Treg cells and induce their differentiation to follicular helper T cells [44].

Therefore, data from previous reports suggest that dyslipidemia contributes to a microenvironment in lesions which is especially hostile for Treg cells, indicating that decreased immunosuppression by Treg cells in atherosclerotic lesions is likely due to local apoptosis and differentiation to T helper cell subsets but not due to decreased migration of circulating Treg cells towards lesions.

Diet-induced dyslipidemia increased the levels of cholesterol and lipid droplets in Treg cells in the spleen, medLN and atherosclerotic lesions of the aorta but not in the blood and iLN. It is unclear whether the increase in lipids in Treg cells from the medLN and atherosclerotic lesions occurred *in situ* or whether Treg cells which accumulated lipids elsewhere preferentially migrated towards atherosclerotic lesions and (subsequently) to draining LNs. Further investigation is required to examine whether Treg cells from atherosclerotic lesions can efficiently migrate towards draining LNs as migration from sites of inflammation towards draining LNs via afferent lymph vessels is regulated in part by CCR7 and S1Pr1 [45].

Regardless of the tissue in which lipid accumulation occurs in Treg cells during dyslipidemia, it is intriguing to investigate whether lipid loaded Treg cells which reside in the microenvironment of atherosclerotic lesions also have altered migratory and metabolic phenotypes and how these contribute to aberrations in their immunomodulatory function and contribute to increased apoptosis and local differentiation.

mTORC2 activity was increased in WTD-Tregs, which, through the mTORC2-Akt-Foxo1-Klf2 axis, resulted in decreased expression of markers which T cells require to home towards LNs. As a result of decreases in expression of CCR7, CD62L and S1Pr1, WTD-Tregs were less able to migrate towards dLNs. These findings confirmed to some extent a report describing obesity-induced metabolic stress causing altered PI3K-p110δ activity which, via increased mTORC2 activity, skews $CD4^+$ T cell migration towards sites of inflammation [19]. As we observed a large increased in FFAs in the serum of WTD-fed mice as compared to NCD-fed mice, it is probable that a feeding *Ldlr*$^{-/-}$ mice a WTD increased circulating palmitate levels as well which altered PI3K and mTORC2 activity in Treg cells through similar mechanisms. Thereby, perturbations in systemic lipid metabolism had profound effects on the migratory markers which WTD-Treg cells express.

Dyslipidemia led to elevated cholesterol in Treg cells which mildly decreased mTORC1 activity and led to decreased expression of genes from the mevalonate pathway without affecting the levels of HIF1α and its transcriptional targets. The effects of diet-induced dyslipidemia on the mevalonate pathway in Treg cells are reminiscent of the effects Treg cell-specific *Raptor* deletion has on cholesterol synthesis [8]. However, the effects we observed were most likely also due to liver-X-receptor (as indicated by increased expression of Abca1 and Abcg1 in WTD-Treg cells) and sterol regulatory element bind-

ing protein (SREBP) directly responding to intracellular cholesterol accumulation to prevent lipotoxicity. In this study, endocytosis of lipoproteins resulted in large amounts of cholesterol in lysosomes which could be sensed by mTORC1. Lysosomal cholesterol accumulation can specifically activate the mTORC1 complex through the SLC38A9–Niemann-Pick C1 signaling complex [46]. Instead, our data suggested cholesterol overload in Treg cells decreased mTORC1 activity. This is also supported by literature describing Treg cell specific genetic deletion of *Abcg1* in mice with normolipidemia and dyslipidemia resulted in an increase in free cholesterol levels and decreased mTORC1 activity in Treg cells [14]. Teleologically, metabolic stress during prolonged dyslipidemia requires a cell intrinsic response to prevent lipotoxicity and decreased lipid synthesis, partly regulated by decreased mTORC1 and SREBP activity, establishes this.

Dyslipidemia increased the mitochondrial FA oxidation rate and reversion to normolipidemia through dietary intervention abolished this effect, which suggested that systemic lipid metabolism is tightly linked to cellular lipid metabolism in Treg cells. Treg cells, which unlike foam cells are not historically recognized as lipid scavengers, adapt their cellular metabolism most likely to prevent lipotoxicity. This had a profound effect on their migratory function. Although glycolysis and glycolytic capacity were slightly impaired, most likely as a result of cholesterol-mediated inhibition of mTORC1 activity, increased ATP generation through FA oxidation might have compensated for these defects when large amounts of ATP are required for cytoskeletal actin rearrangements during cell migration [47,48]. In Treg cells, glucokinase has been shown to be crucial for glycolysis-derived ATP generation to facilitate Treg cell migration upon migratory stimuli [12]. However, the Treg cells used in that report were primarily generated or treated *in vitro* meaning that these cells probably depended mainly on glycolysis to generate ATP. In support of this, in $CD8^+$ T cells, the ECAR dose-dependently increases with the concentration of glucose in the culture medium [49]. As dyslipidemia and GW501516 treatment augmented FA oxidation and migration but not glycolysis in Treg cells, our study suggests that the dominant ATP-generating catabolic pathway is crucial for Treg cell migration and how bioenergetic metabolism is skewed by which environmental stimuli determines which catabolic pathway is dominant.

Treatment of Treg cells with GW501516 resulted in higher migratory capacity of Treg cells towards sites of inflammation. As this was dependent on FA oxidation both *in vitro* and *in vivo*, treatment with this compound presumably decreased the metabolic flexibility of Treg cells. In contrast, pre-treatment of WTD-Tregs with etomoxir only showed mild effects on their migratory capacity, suggesting that WTD-Treg cells were better capable of switching to alternative catabolic pathways to generate ATP. Further characterization of the dependence of WTD-Treg cells on other metabolic pathways besides glycolysis and FA oxidation would deepen our understanding of how dyslipidemia can affect Treg

cell metabolism, possibly leading to new therapeutic opportunities to modulate Treg cell function and dampen inflammation.

Altogether, our observations suggest that dietary lipids can alter Treg cell metabolism and migratory function. It is expected that pharmacological intervention to increase Treg cell migration alone will not suffice to dampen atherosclerosis or other autoimmune-like diseases if the microenvironment at the site of inflammation is not suitable for Treg cells. Furthermore, our findings suggest that in other metabolic diseases which are characterized by nutrient excess and autoimmune-like chronic inflammation (such as obesity) cellular metabolism in T(reg) cells might be altered and that these adaptations might be exploited to alter their migration for therapeutic purposes.

REFERENCES

1. Libby, P., Lichtman, A. H. & Hansson, G. K. Immune Effector Mechanisms Implicated in Atherosclerosis: From Mice to Humans. *Immunity* 38, 1092–1104 (2013).
2. Buckner, J. H. Mechanisms of impaired regulation by CD4+CD25+FOXP3+ regulatory T cells in human autoimmune diseases. *Nat. Rev. Immunol.* 10, 849–859 (2010).
3. von Boehmer, H. & Daniel, C. Therapeutic opportunities for manipulating TReg cells in autoimmunity and cancer. *Nat. Rev. Drug Discov.* 12, 51–63 (2012).
4. Maganto-Garcia, E., Tarrio, M. L., Grabie, N., Bu, D. -x. & Lichtman, A. H. Dynamic Changes in Regulatory T Cells Are Linked to Levels of Diet-Induced Hypercholesterolemia. *Circulation* 124, 185–195 (2011).
5. de Boer, O. J., van der Meer, J. J., Teeling, P., van der Loos, C. M. & van der Wal, A. C. Low Numbers of FOXP3 Positive Regulatory T Cells Are Present in all Developmental Stages of Human Atherosclerotic Lesions. *PLoS ONE* 2, e779 (2007).
6. Dietel, B. *et al.* Decreased numbers of regulatory T cells are associated with human atherosclerotic lesion vulnerability and inversely correlate with infiltrated mature dendritic cells. *Atherosclerosis* 230, 92–99 (2013).
7. Mor, A., Luboshits, G., Planer, D., Keren, G. & George, J. Altered status of CD4+CD25+ regulatory T cells in patients with acute coronary syndromes. *Eur. Heart J.* 27, 2530–2537 (2006).
8. Zeng, H. *et al.* mTORC1 couples immune signals and metabolic programming to establish T(reg)-cell function. *Nature* 499, 485–490 (2013).
9. Procaccini, C. *et al.* The Proteomic Landscape of Human Ex Vivo Regulatory and Conventional T Cells Reveals Specific Metabolic Requirements. *Immunity* 44, 406–421 (2016).
10. Michalek, R. D. *et al.* Cutting Edge: Distinct Glycolytic and Lipid Oxidative Metabolic Programs Are Essential for Effector and Regulatory CD4+ T Cell Subsets. *J. Immunol.* 186, 3299–3303 (2011).
11. De Rosa, V. *et al.* Glycolysis controls the induction of human regulatory T cells by modulating the expression of FOXP3 exon 2 splicing variants. *Nat. Immunol.* (2015). doi:10.1038/ni.3269
12. Kishore, M. *et al.* Regulatory T Cell Migration Is Dependent on Glucokinase-Mediated Glycolysis. *Immunity* 47, 875-889.e10 (2017).
13. Shen, Y. *et al.* Metabolic control of the scaffold protein TKS5 in tissue-invasive, proinflammatory T cells. *Nat. Immunol.* (2017). doi:10.1038/ni.3808
14. Cheng, H.-Y. *et al.* Loss of ABCG1 influences regulatory T cell differentiation and atherosclerosis. *J. Clin. Invest.* (2016). doi:10.1172/JCI83136
15. Shi, L. Z. *et al.* HIF1alpha-dependent glycolytic pathway orchestrates a metabolic checkpoint for the differentiation of TH17 and Treg cells. *J. Exp. Med.* 208, 1367–76 (2011).
16. Wang, R. *et al.* The transcription factor Myc controls metabolic reprogramming upon T lymphocyte activation. *Immunity* 35, 871–82 (2011).
17. DeBerardinis, R. J., Lum, J. J. & Thompson, C. B. Phosphatidylinositol 3-Kinase-dependent Modulation of Carnitine Palmitoyltransferase 1A Expression Regulates Lipid Metabolism during Hematopoietic Cell Growth. *J. Biol. Chem.* 281, 37372–37380 (2006).
18. Um, S. H. *et al.* Absence of S6K1 protects against age-and diet-induced obesity while enhancing insulin sensitivity. *Nature* 431, 200–205 (2004).
19. Mauro, C. *et al.* Obesity-Induced Metabolic Stress Leads to Biased Effector Memory CD4 + T Cell Differentiation via PI3K p110δ-Akt-Mediated Signals. *Cell Metab.* 25, 593–609 (2017).
20. Goldstein, J. L. & Brown, M. S. The LDL Receptor. *Arterioscler. Thromb. Vasc. Biol.* 29, 431–438 (2009).

21. Zhang, N. *et al.* Regulatory T Cells Sequentially Migrate from Inflamed Tissues to Draining Lymph Nodes to Suppress the Alloimmune Response. *Immunity* 30, 458–469 (2009).
22. Chi, H. Regulation and function of mTOR signalling in T cell fate decisions. *Nat. Rev. Immunol.* (2012). doi:10.1038/nri3198
23. Palinski, W. *et al.* Cloning of monoclonal autoantibodies to epitopes of oxidized lipoproteins from apolipoprotein E-deficient mice. Demonstration of epitopes of oxidized low density lipoprotein in human plasma. *J. Clin. Invest.* 98, 800–814 (1996).
24. Klingenberg, R. *et al.* Intranasal Immunization With an Apolipoprotein B-100 Fusion Protein Induces Antigen-Specific Regulatory T Cells and Reduces Atherosclerosis. *Arterioscler. Thromb. Vasc. Biol.* 30, 946–952 (2010).
25. Peterson, T. R. *et al.* mTOR Complex 1 Regulates Lipin 1 Localization to Control the SREBP Pathway. *Cell* 146, 408–420 (2011).
26. Düvel, K. *et al.* Activation of a Metabolic Gene Regulatory Network Downstream of mTOR Complex 1. *Mol. Cell* 39, 171–183 (2010).
27. Sun, Q. *et al.* Mammalian target of rapamycin up-regulation of pyruvate kinase isoenzyme type M2 is critical for aerobic glycolysis and tumor growth. *Proc. Natl. Acad. Sci.* 108, 4129–4134 (2011).
28. Cunningham, J. T. *et al.* mTOR controls mitochondrial oxidative function through a YY1–PGC-1α transcriptional complex. *Nature* 450, 736–740 (2007).
29. Raud, B. *et al.* Etomoxir Actions on Regulatory and Memory T Cells Are Independent of Cpt1a-Mediated Fatty Acid Oxidation. *Cell Metab.* (2018). doi:10.1016/j.cmet.2018.06.002
30. Libby, P. Inflammation and Atherosclerosis. *Circulation* 105, 1135–1143 (2002).
31. Foks, A. C. *et al.* Differential effects of regulatory T cells on the initiation and regression of atherosclerosis. *Atherosclerosis* 218, 53–60 (2011).
32. Foks, A. C. *et al.* Interruption of the OX40-OX40 Ligand Pathway in LDL Receptor-Deficient Mice Causes Regression of Atherosclerosis. *J. Immunol.* 191, 4573–4580 (2013).
33. Bensinger, S. J. & Tontonoz, P. Integration of metabolism and inflammation by lipid-activated nuclear receptors. *Nature* 454, 470–7 (2008).
34. Berger, J. & Moller, D. E. The mechanisms of action of PPARs. *Annu. Rev. Med.* 53, 409–435 (2002).
35. Fan, W. *et al.* PPARδ Promotes Running Endurance by Preserving Glucose. *Cell Metab.* 25, 1186-1193.e4 (2017).
36. Cipolletta, D. *et al.* PPAR-γ is a major driver of the accumulation and phenotype of adipose tissue Treg cells. *Nature* (2012). doi:10.1038/nature11132
37. Nahlé, Z. *et al.* CD36-dependent Regulation of Muscle FoxO1 and PDK4 in the PPARδ/β-mediated Adaptation to Metabolic Stress. *J. Biol. Chem.* 283, 14317–14326 (2008).
38. Chawla, A. *et al.* PPARδ is a very low-density lipoprotein sensor in macrophages. *Proc. Natl. Acad. Sci.* 100, 1268–1273 (2003).
39. Kahremany, S., Livne, A., Gruzman, A., Senderowitz, H. & Sasson, S. Activation of PPARδ: from computer modelling to biological effects: Binding parameters of PPARδ activators. *Br. J. Pharmacol.* 172, 754–770 (2015).
40. Klingler, C. *et al.* Lysophosphatidylcholines activate PPARδ and protect human skeletal muscle cells from lipotoxicity. *Biochim. Biophys. Acta BBA - Mol. Cell Biol. Lipids* 1861, 1980–1992 (2016).
41. Zhang, W. *et al.* Impaired Thymic Export and Increased Apoptosis Account for Regulatory T Cell Defects in Patients with Non-ST Segment Elevation Acute Coronary Syndrome. *J. Biol. Chem.* 287, 34157–34166 (2012).
42. Jia, L. *et al.* Methylation of FOXP3 in regulatory T cells is related to the severity of coronary artery disease. *Atherosclerosis* 228, 346–352 (2013).

43. Li, J. *et al.* CCR5+ T-bet+ FoxP3+ Effector CD4 T Cells Drive Atherosclerosis. *Circ. Res.* CIRCRE-SAHA–116 (2016).
44. Gaddis, D. E. *et al.* Apolipoprotein AI prevents regulatory to follicular helper T cell switching during atherosclerosis. *Nat. Commun.* 9, (2018).
45. Hunter, M. C., Teijeira, A. & Halin, C. T Cell Trafficking through Lymphatic Vessels. *Front. Immunol.* 7, (2016).
46. Castellano, B. M. *et al.* Lysosomal cholesterol activates mTORC1 via an SLC38A9–Niemann-Pick C1 signaling complex. *Science* 355, 1306–1311 (2017).
47. Bernstein, B. W. & Bamburg, J. R. Actin-ATP hydrolysis is a major energy drain for neurons. *J. Neurosci.* 23, 1–6 (2003).
48. Pantaloni, D., Le Clainche, C. & Carlier, M.-F. Mechanism of actin-based motility. *Science* 292, 1502–1506 (2001).
49. Blagih, J. *et al.* The Energy Sensor AMPK Regulates T Cell Metabolic Adaptation and Effector Responses In Vivo. *Immunity* 42, 41–54 (2015).
50. Fu, H. *et al.* Self-recognition of the endothelium enables regulatory T-cell trafficking and defines the kinetics of immune regulation. *Nat. Commun.* 5, (2014).
51. Hu, C. *et al.* RPLC-Ion-Trap-FTMS Method for Lipid Profiling of Plasma: Method Validation and Application to p53 Mutant Mouse Model. *J. Proteome Res.* 7, 4982–4991 (2008).
52. Strassburg, K. *et al.* Quantitative profiling of oxylipins through comprehensive LC-MS/MS analysis: application in cardiac surgery. *Anal. Bioanal. Chem.* 404, 1413–1426 (2012).

SUPPLEMENTARY FIGURES

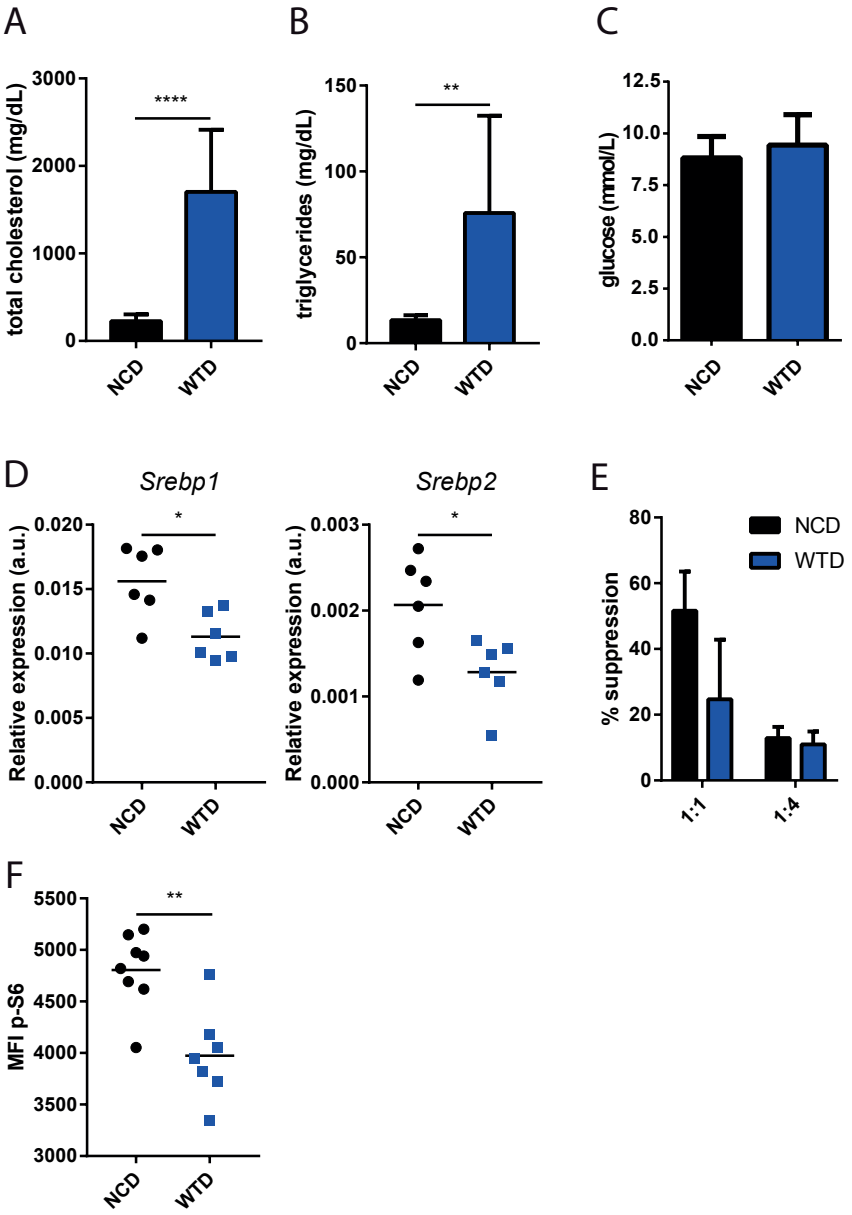

Figure S1 Diet-induced dyslipidemia affects mTORC1 signaling and cholesterol metabolism (A) Total cholesterol levels in serum (B) Triglyceride levels in serum (C) Blood glucose levels after 4h of fasting (D) *Srebp1* and *Srebp2* in isolated Treg cells. (E) Suppression assay with Treg cells and effector T cells in two different ratios (Treg cell:splenocytes) (F) mTORC1 activity in conventional T cells as measured by assessing p-S6 levels. Data in A-D and F are representative for two individual experiments. Data in E represents one experiment. Data in A-C and E represent mean ± standard deviation. *p<0.05, **p<0.01, ****p<0.0001.

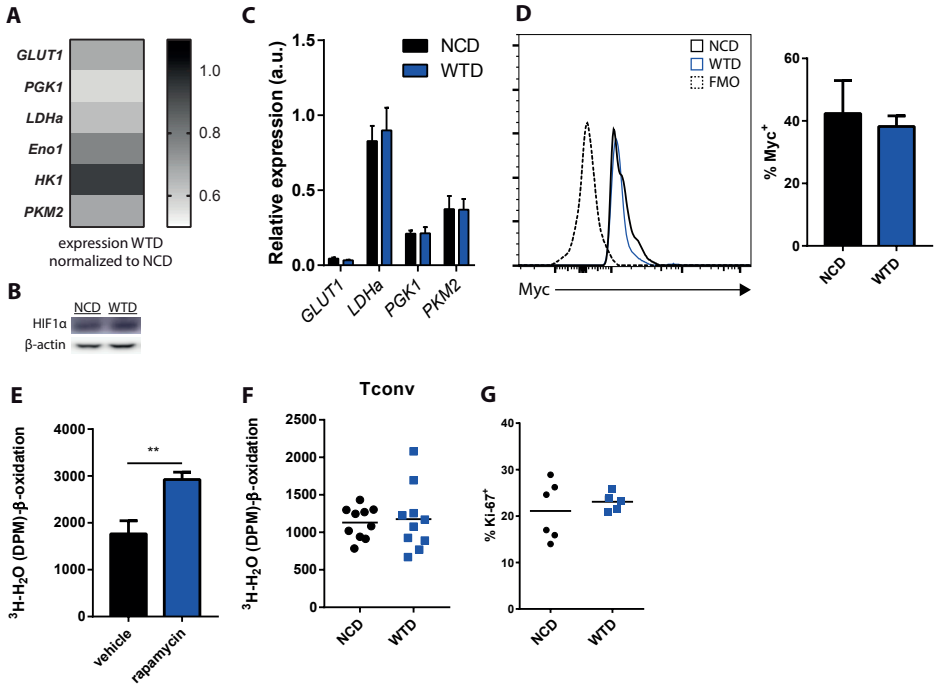

Figure S2 Metabolic effects of mTOR inhibition (A) Expression of HIF1α targets in Treg cells cultured with NCD- or WTD-serum. (B) HIF1α immunoblot on freshly isolated NCD- or WTD-Treg cells. (C) Expression of HIF1α targets in NCD- and WTD-Treg cells (D) Myc expression in NCD- and WTD-Treg cells (E) FA oxidation in Treg cells after rapamycin treatment (F) ^{3}H-palmitic acid detritiation in conventional T (Tconv) cells from NCD- or WTD-fed *Ldlr*$^{-/-}$ mice. (G) Percentage of proliferating Treg cells. **p<0.01. The data in C-E represent the mean±standard deviation.

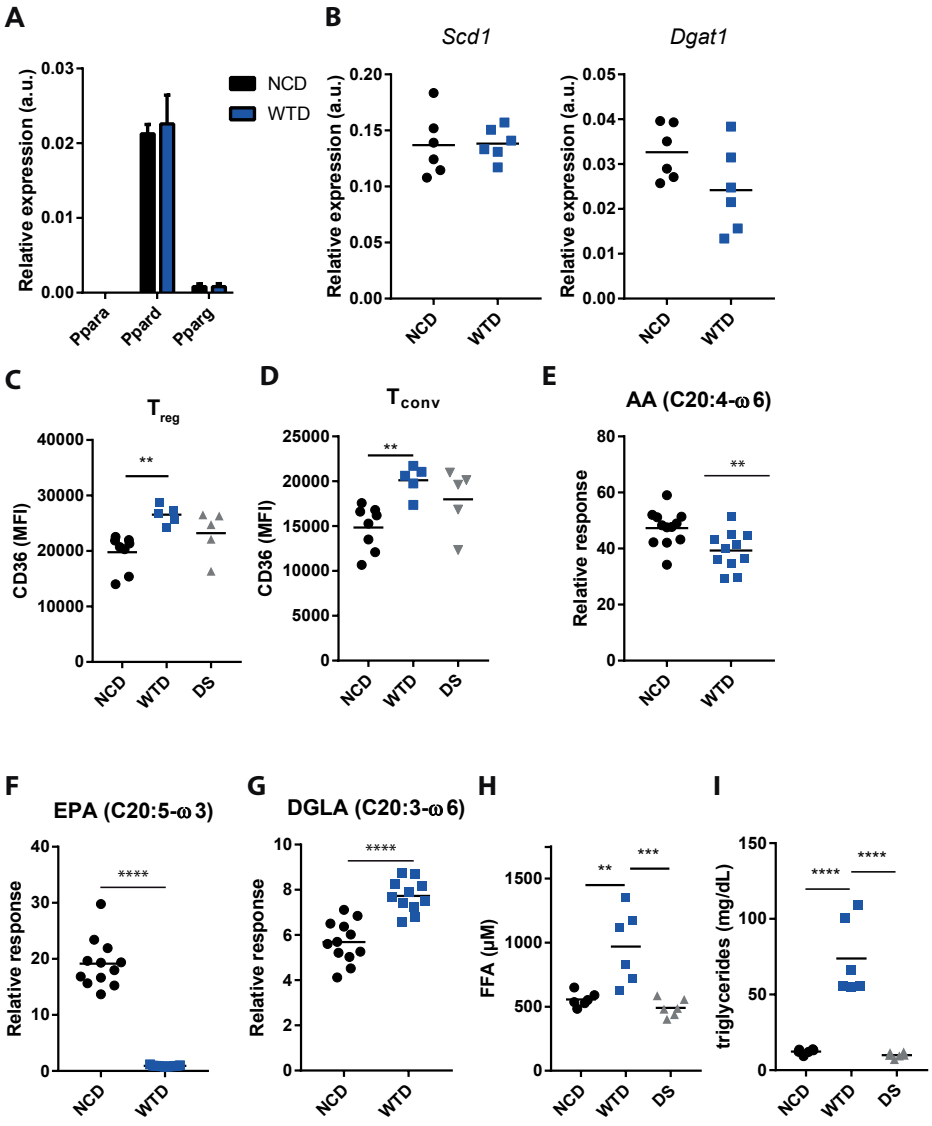

Figure S3 PPAR ligands and target gene expression during diet-induced dyslipidemia. (A) Expression of different PPARs in NCD-Treg cells and WTD-Treg cells. (B) Expression of the PPAR γ target genes *Scd1* and *Dgat1* (C) CD36 expression (MFI) in Treg cells from diet switch experiments (D) CD36 expression (MFI) in Tconv cells from diet switch experiments (E) Relative abundance of arachidonic acid (AA) (F) eicosapentaenoic acid (EPA) and (G) dihomo-γ-linolenic acid (DGLA) in serum of *Ldlr*$^{-/-}$ mice fed an NCD or WTD. (H) Free fatty acid (FFA) levels in serum during diet switch experiments (I) Serum triglyceride levels in the serum**.** *p<0.05, **p<0.01, ***p<0.001, ****p<0.0001. The data in A represents the mean±standard deviation.

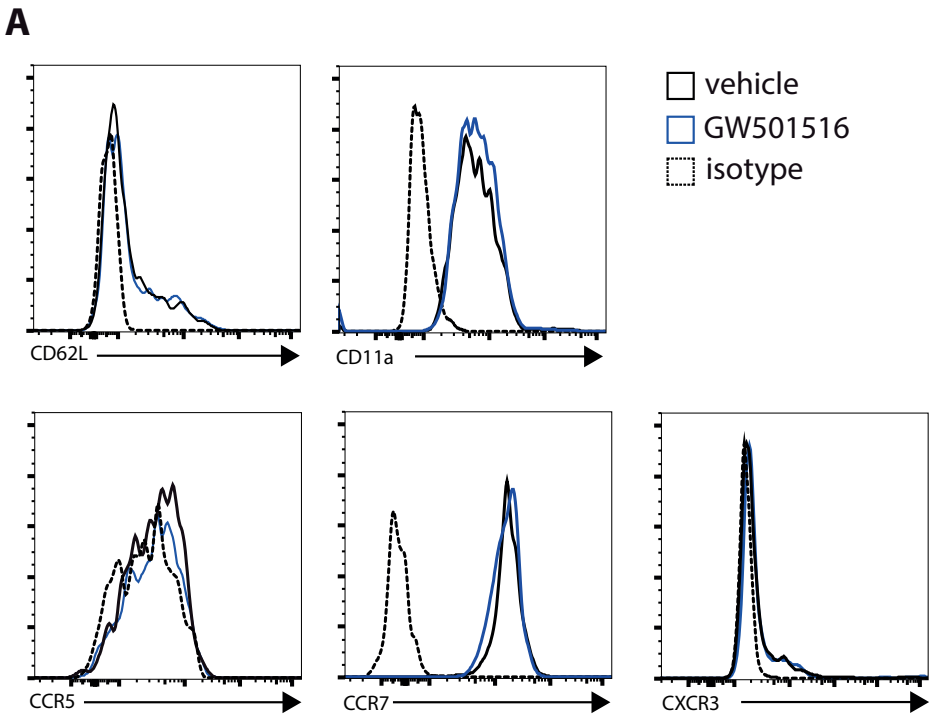

Figure S4 GW501516 treatment and migratory markers. (A) *In vitro* treatment of Treg cells with GW501516 did not affect the expression of CD62L, CD11a (also known as lymphocyte function-associated antigen 1, or LFA1), C-C chemokine receptor type 5 (CCR5), CCR7 or C-X-C motif receptor 3 (CXCR3).

SUPPLEMENTARY TABLES

Table 1 Antibodies/dyes used for flow cytometry

antigen	label	clone	manufacturer
p-4-EBP1 Thr37/46	AF647	236B4	Cell Signaling Technology
CCR5	PE-Cy7	HM-CCR5	BioLegend
CCR7	APC	4B12	eBioscience
CD11a	BV650	2D7	BD Biosciences
CD25	FITC	PC61.5	eBioscience
CD25	APC	PC61.5	eBioscience
CD3	APC	145-2C11	eBioscience
CD36	PE	CRF D-2712	BD Biosciences
CD4	FITC	GK1.5	eBioscience
CD4	PE	GK1.5	eBioscience
CD4	eFluor 405	GK1.5	eBioscience
CD45.1	PB	A20	eBioscience
CD45.2	APC	104	eBioscience
CD62L	PerCP-Cy5.5	MEL-14	eBioscience
CXCR3	PE	CXCR3-173	BioLegend
FoxP3	eFluor 405	FJK-16s	eBioscience
FoxP3	APC	FJK-16s	eBioscience
FoxP3	PE	NRRF-30	eBioscience
Ki-67	FITC	SolA15	eBioscience
p-Akt Ser473	V450	M89-61	BD Biosciences
p-S6 Ser235/236	AF488	2F9	Cell Signaling Technology
Thy1.2	PE-Cy7	53-2.1	eBioscience
eFluor 780 viability dye	APC-Cy7	-	eBioscience

Table 2 List of primers used for qRT-PCR

Gene	Forward primer (5′-3′)	Reverse primer (3′-5′)
Hmgcs1	aaaacacagaaggacttacgcccgg	gttgcagggagtcttggcactttct
Hmgcr	cgagccacgacctaatgaagaatg	tgcatcactaaggaactttgcacc
Idi1	cattggtgtgaagcgagcagcaaag	caccccagataccatcagattgggc
Fdft1	aacatgcctgccgtcaaagctatca	gcttgatgatgggtctgagttgggg
Sqle	gagtgtgtgaccggtcctgttgg	actgaaaagggcccgtggttttgta
Srebp1	tctgaggaggagggcaggttcca	ggaaggcaggggggcagatagca
Srebp2	ccagctcctgggtgagacctac	caggcgcacagtggcttcat
Abca1	agagcaaaaagcgactccacatagaa	cggccacatccacaactgtct
Abcg1	ttgacaccatcccagcctac	cagtgcaggtcttctcggt
Klf2	gccgccacacatacttgcagct	tccagccgcatccttcccagtt
CD62L	tcattcctgtagccgtcatggtc	agcacttcatggctttcctttcac
Ccr7	cgtgctggtggtggctctcct	accgtggtattctcgccgatgtagtc
S1pr1	gtcagtcgccgacagcagcaag	acagcaaagccaggtcagcgag
Hif1a	aggagccttaacctgtctgccac	cctgctgcttgaaaaagggagcc
Glut1	ggtgtgcagcagcctgtgt	cacagtgaaggccgtgttga
Pgk1	gtgggtcgagctaagcagattgtttgg	tgctcacatggctgactttatcctctgt
Ldha	acgtggcttggaaaatcagtggctt	ggcaacattcacaccactccacaca
Eno1	cgcctggccaagtacaatcagatcc	tctccggtccatgctttatttggcc
Hk1	acgggacgctctacaaactccatc	gaggaaggacacggtacactttggt
Pkm2	ccattaccagcgaccccacagaag	agacttggtgagcacgataatggcc
Cpt1a	ggttgctgatgacggctatggt	tggcttgtctcaagtgcttccc
Ppara	tgacatttccctgtttgtggctgct	tgcacaatcccctcctgcaacttc
Ppard	gaccagaacacacgcttccttc	ccgacattccatgttgaggctg
Pparg	aagccctttggtgactttatggagcc	tgcagcaggttgtcttggatgtcc
Slc25a20	cagagatgtgttgagagagctgatccg	tgtccagcatccacaggtcttgaag
Plin2	gcacagtgccaaccagaaaattcagg	cagtctggcatgtagtctggagctg
Lipe	ctgacaataaaggacttgagcaactc	aggccgcagaaaaaagttgac
Taf7	agtctgggcatgtcaacctgaa	cgtaacacaaggcaaatcgacca
actin	cttctttgcagctccttcgttgccg	aatacagcccggggagcatcgtc
Rpl27	cgccaagcgatccaagatcaagtcc	agctgggtccctgaacacatccttg
Rpl37	agagacgaaacactaccgggactgg	cttgggtttcggcgttgttccctc
36B4	ctgagtacaccttcccacttactga	cgactcttcctttgcttcagcttt